REPORT DOCUMENTATION PAGE

Form Approved OMB No. 0704-0188

1. REPORT DATE *(DD-MM-YYYY)*	2. REPORT TYPE	3. DATES COVERED *(From – To)*
28-04-2009	Final Report	1 May 2005 - 26-Aug-09

4. TITLE AND SUBTITLE

Phase-locked Optical Signal Recovery

5a. CONTRACT NUMBER
FA8655-05-1-3035

5b. GRANT NUMBER

5c. PROGRAM ELEMENT NUMBER

6. AUTHOR(S)

Professor Alwyn J Seeds

5d. PROJECT NUMBER

5d. TASK NUMBER

5e. WORK UNIT NUMBER

7. PERFORMING ORGANIZATION NAME(S) AND ADDRESS(ES)
University College London
Torrington Place
London WC1E 7JE
United Kingdom

8. PERFORMING ORGANIZATION REPORT NUMBER
N/A

9. SPONSORING/MONITORING AGENCY NAME(S) AND ADDRESS(ES)

EOARD
Unit 4515 BOX 14
APO AE 09421

10. SPONSOR/MONITOR'S ACRONYM(S)

11. SPONSOR/MONITOR'S REPORT NUMBER(S)
Grant 05-3035

12. DISTRIBUTION/AVAILABILITY STATEMENT

Approved for public release; distribution is unlimited.

13. SUPPLEMENTARY NOTES

14. ABSTRACT

Phase-locked receivers have long been used for the recovery of signals in low signal to noise ratio (SNR) environments, such as space applications. A loop for use with semiconductor laser generated signals would require a bandwidth of >500 MHz for low phase error variance (<0.01 rad2) tracking, constraining the propagation delay to <0.3 ns. Since this requires an equivalent path length of <100 mm, conventional realizations in optical fiber technology are not possible, requiring special micro-optical solutions. An alternative technique is to use optical injection locking. This avoids loop propagation limitations, but stable locking ranges are typically <1 GHz, requiring precision (<10 mK) control of the receiver laser and continuous adjustment to track drift in the incoming signal. At University College London (UCL), we have developed a technique that overcomes the limitations described above-the Optical Injection Phase Lock Loop (OIPLL) in which a narrow bandwidth optical phase lock loop (OPLL) is used to control the free-running frequency of an optically injection locked laser to compensate for thermal drift, drift in the incoming signal and low-frequency noise. If successful this would enable low SNR optical signals to be recovered without the need for constant skilled adjustment of the receiver system. For the feasibility study we propose to investigate two possible detection schemes. The first is an homodyne OIPLL. Although this appears simple in principle there are significant challenges in implementation. The second scheme is based on heterodyne detection, with the heterodyne frequency chosen to be remote from data modulation interference. In this approach, the incoming signal passes through a modulator, where it is sinusoidally intensity modulated at microwave frequency by the offset source. The slave laser is injection locked to one of these side frequencies through an optical circulator. The output from the slave laser, containing both the locked signal and residual input signal passes back through the circulator to the photodiode where the heterodyne between input and slave laser output is detected and then compared with the offset frequency in a microwave phase detector. The phase detector output, processed by the loop filter tunes the slave laser.

15. SUBJECT TERMS
EOARD, Heterodyne Detection, Optical sensing, Laser Measurements Techniques

16. SECURITY CLASSIFICATION OF:			17. LIMITATION OF ABSTRACT	18, NUMBER OF PAGES	19a. NAME OF RESPONSIBLE PERSON
a. REPORT	b. ABSTRACT	c. THIS PAGE			A. GAVRIELIDES
UNCLAS	UNCLAS	UNCLAS	UL	52	19b. TELEPHONE NUMBER *(Include area code)* +44 (0)1895 616205

UCL DEPARTMENT OF ELECTRONIC &

PHASE-LOCKED OPTICAL SIGNAL RECOVERY

Award number
FA8655-05-1-3035

Final Report
January 2009

Martyn Fice
Alwyn Seeds

ABSTRACT

The concept, design, implementation and experimental evaluation of a novel homodyne coherent optical receiver are described. The receiver uses an Optical Injection Phase Lock Loop (OIPLL) for carrier recovery, which combines optical injection locking with low-bandwidth electronic feedback to give a low-delay, wide-bandwidth optical phase lock loop (OPLL) with large tracking range. The large effective loop bandwidth provided by the optical injection locking (typically around 1 GHz) far exceeds that obtainable with conventional OPLLs, enabling locking with very low phase error to be achieved, even with combined laser linewidths in the MHz region. The electronic feedback tracks low frequency noise, thermal drift of the injection-locked laser, and frequency drift of the incoming signal.

This report consolidates and summarises in a single document work carried out on the homodyne OIPLL receiver in several phases of the project. It includes new material from the final phase of the project (Phase 4).

Overall, through the course of the project, we have demonstrated the following key features and attributes of the OIPLL coherent receiver:

- Demodulation of both binary amplitude shift keying (ASK) and binary phase shift keying (PSK) data at 10 Gb/s.
- Low bit error ratio (BER) operation ($<10^{-10}$) at high optical signal-to-noise ratio (OSNR) for signal and local oscillator lasers with linewidths in the MHz range.
- Performance close to the theoretical limit at low OSNR, where BER is determined by beating between the local oscillator laser and amplified spontaneous emission optical noise.
- Lower required OSNR with binary ASK compared to direct detection.
- Fibre dispersion OSNR penalty for binary ASK similar to direct detection.
- Frequency selective operation due to high rejection of common mode signals, enabling selection of closely spaced wavelength division multiplexing (WDM) signals without optical filtering.
- Large tracking range, greater than the frequency stability of the source lasers used in dense WDM optical transmission systems.
- Very low linewidth-related phase error, which should give negligible penalty in the absence of other implementation-dependent sources of phase error.

COMPLIANCE WITH GRANT TERMS

Acknowledgement of Sponsorship

The Grantee accepts responsibility for assuring that an acknowledgement of Government support will appear in any publication of any material based on or developed under this project, in the following terms:

"Effort sponsored by the Air Force Office of Scientific Research, Air Force Material Command, USAF, under grant number FA8655-05-1-3035. The U.S. Government is authorized to reproduce and distribute reprints for Government purpose notwithstanding any copyright notation thereon."

Disclaimer

The Grantee accepts responsibility for assuring that every publication of material based on or developed under this project contains the following disclaimer:

"The views and conclusions contained herein are those of the author and should not be interpreted as necessarily representing the official policies or endorsements, either expressed or implied, of the Air Force Office of Scientific Research or the U.S. Government."

Disclosure of inventions

The Grantee certifies that there were no subject inventions to declare during the performance of this grant.

CONTENTS

LIST OF FIGURES

1 INTRODUCTION

The objective of this project was to investigate and demonstrate techniques for the demodulation by coherent optical detection of an optical data signal typical of those used in high data rate (e.g. 10 Gb/s) commercial communications systems. The key technique studied was the generation of an optical carrier that is phase locked to that of the optical data signal.

In Phase 1 of the project (May 2005 to April 2006), the feasibility of using a technique known as the Optical Injection Phase Lock Loop (OIPLL) to achieve this was investigated. In Phase 2 (August 2006 to July 2007), demodulation of a 10 Gb/s intensity modulated (or amplitude shift keyed [ASK]) data signal was demonstrated experimentally using a coherent homodyne optical receiver employing carrier phase locking by the OIPLL technique. In Phase 3 (August 2007 to January 2008) and Phase 4 (July 2008 to December 2008) further investigations of the OIPLL receiver have been carried out, including a comparison of its performance against direct detection; a study of its performance as a frequency selective receiver; investigation of its operation following transmission over standard single mode optical fibre; demonstration of a modified phase locking scheme that allows detection of phase modulated signals; and a study of the impact of the transmitter linewidth on the receiver's performance.

This report consolidates into a single document material from Phases 2 to 4 of the project, which relate to the implementation and performance of the homodyne OIPLL receiver. Preliminary work carried out on an heterodyne scheme in Phase 1 of the project was reported in detail at the end of that phase, so has not been reproduced here.

New results obtained in Phase 4 of the project are to be found in Sections 4.4, 4.5 and 4.6 of this report.

2 BACKGROUND

Synchronous demodulation (Figure 1) is a fundamental technique of enormous practical importance in radio communications. Its optical equivalent – often referred to as coherent optical detection – has been extensively investigated since the 1980s, but only in the last few years has it been implemented in commercial telecommunication systems, which until this time have relied instead on the direct detection of intensity modulated signals.

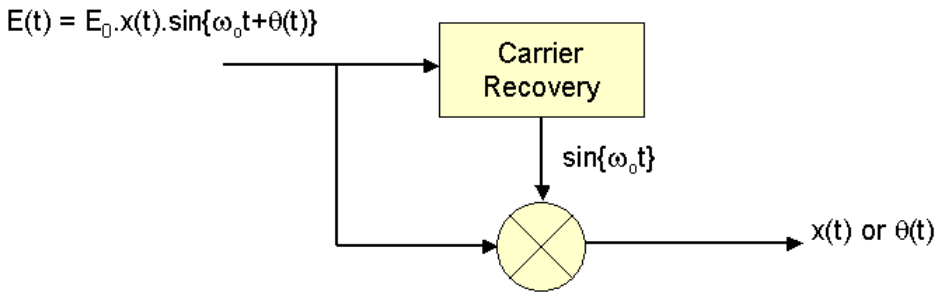

Figure 1: Synchronous demodulation.

Depending on the scenario, coherent optical detection offers the advantages of higher sensitivity, frequency selectivity, and higher channel capacity through the use of more complex modulation formats. The incoming optical signal is combined with an optical carrier (the „local oscillator') on a photo-detector, producing an electrical signal at the difference frequency between the signal and local oscillator (LO) with amplitude proportional to the product of their electric fields.

If the signal and LO have the same frequency and are phase locked (homodyne receiver), synchronous coherent demodulation direct to the baseband occurs. This is considerably less complex – in principle – than the alternative heterodyne receiver architecture, in which the signal and LO differ in frequency, so demodulating the data to an intermediate frequency (typically in the RF or microwave bands), before demodulation to baseband in the electrical domain by synchronous demodulation or by envelope detection. However, implementing an optical phase lock loop (OPLL) to generate the synchronised carrier for the homodyne technique requires narrow laser linewidths and low propagation delay loops (Figure 2). One approach to circumventing this problem is to use a free-running LO and digitise the detected signal using a very fast analogue-to-digital converter (≥ 10 GSamples/s). In this "digital coherent" approach [1], which is currently being extensively researched and has recently been commercialised, frequency and phase errors can be tracked and corrected using digital signal processing (DSP) techniques on the digitised signal. Transmission impairments, such as chromatic and polarisation mode dispersion, can also be corrected using DSP.

In this project, however, we have investigated an alternative to the conventional OPLL in order to recover data directly without the need for digitisation and DSP. This approach may find application in scenarios where the digital coherent technique is considered too expensive or power hungry, but might equally be used as part of a digital coherent receiver to simplify the DSP requirements (by eliminating the frequency and phase tracking elements) or to ease the stringent linewidth requirements of some complex modulation formats. The Optical Injection Phase Lock Loop (OIPLL) technique invented at University College London (UCL) overcomes the limitations of the conventional OPLL by combining optical injection locking of a laser with a relatively low-bandwidth OPLL [2]. Reduction of phase noise at large offsets from the carrier is achieved mainly through the injection locking mechanism, while the OPLL tracks low frequency noise, thermal drift of the injection-locked laser, and frequency drift of the incoming signal.

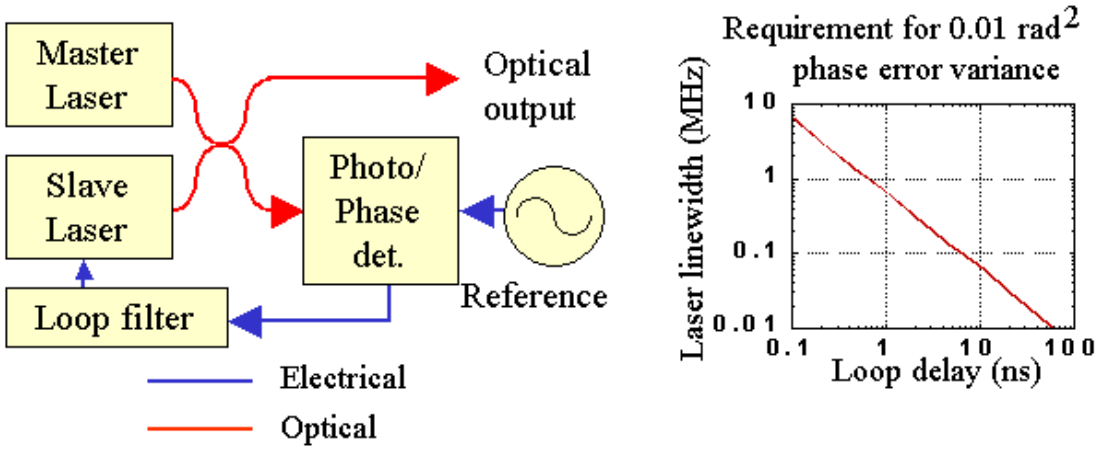

Figure 2: Optical phase lock loop.

In order to use the OIPLL to recover data, the recovered phase-locked carrier must be combined with a portion of the master signal and detected. A scheme for combining the phase recovery OIPLL with the data demodulation path is shown conceptually in Figure 3.

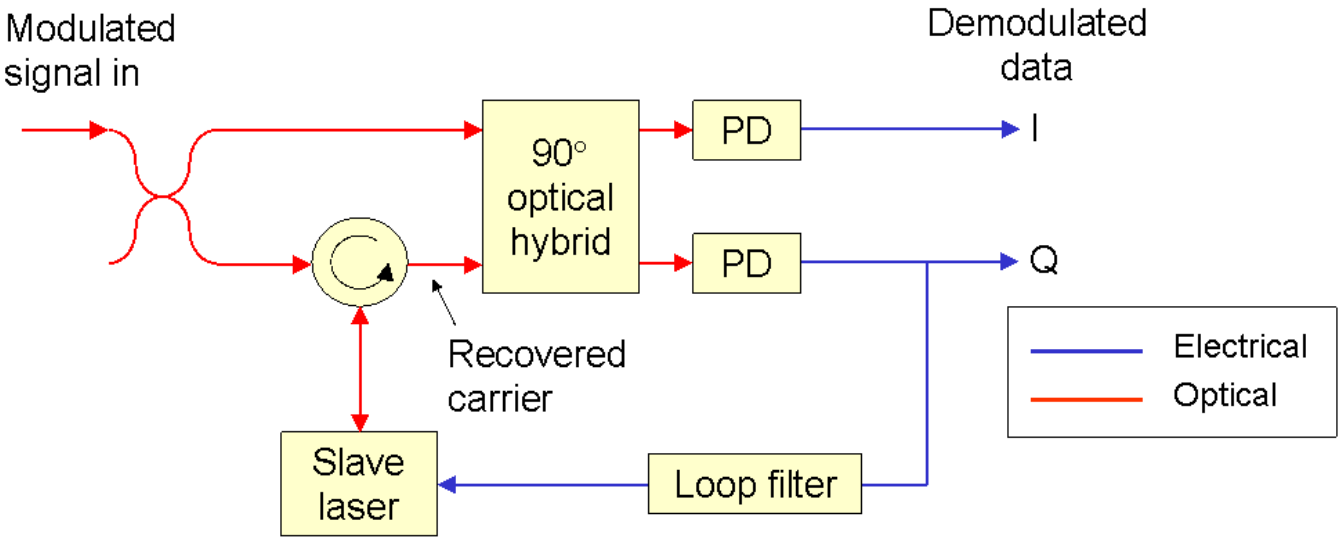

Figure 3: OIPLL receiver concept.

A portion of the input signal is tapped off and used to injection lock the slave laser (LO), providing a recovered carrier which is phase locked to the input signal. The input signal and LO are combined in a quadrature (90°) optical hybrid, one output of which gives the demodulated data, while the quadrature channel forms part of the optical phase lock loop (OPLL), which ensures that the slave laser remains locked to the incoming signal.

3 METHODS, ASSUMPTIONS, AND PROCEDURES

3.1 Experimental OIPLL receiver

The configuration of the experimental OIPLL receiver is shown in Figure 4.

The optical hybrid used was a lithium niobate integrated optics device from CeLight Inc. (CL-QOH-90). The splitting ratios of the four optical couplers and values of the two phase shifters on this component are all electrically adjustable, giving considerable flexibility to its set up and operation, for instance allowing very high common mode rejection ratio to be obtained with balanced detectors by careful adjustment of the splitting ratio of the output couplers. The excess loss of the optical hybrid (i.e. excluding the splitting losses in the couplers) was about 6 dB. Balanced photo-detectors from Discovery Semiconductors were used on both outputs. The data output (I channel) used a balanced photo-receiver (DSC-R405ER) with an integral AC-coupled RF amplifier, with an electrical bandwidth of around 18 GHz. The control loop required DC coupling, so a balanced photodiode pair (DSC730) was used on the Q channel. The bandwidth of these photodiodes is around 30 GHz, although for deriving the control signal only low speed (MHz bandwidth) components are necessary.

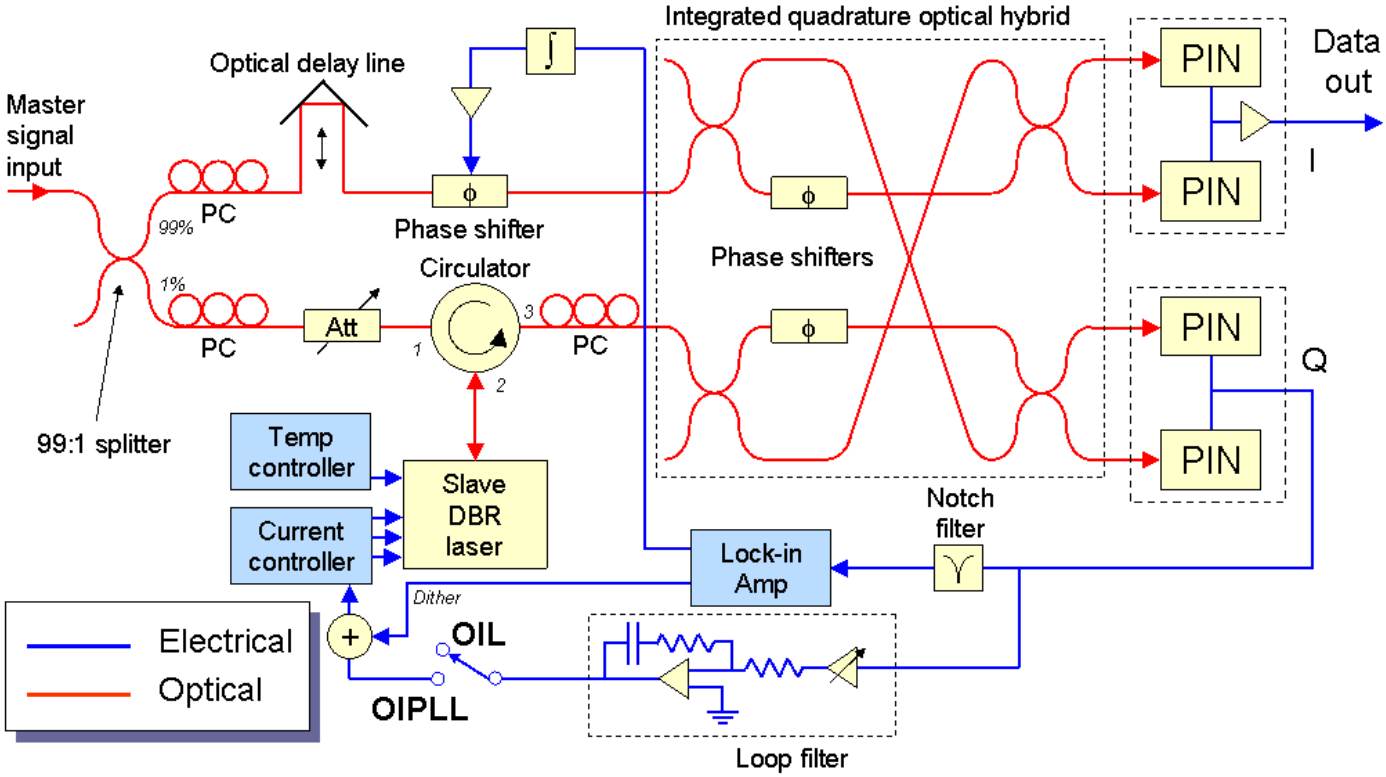

Figure 4: OIPLL receiver with integrated optics quadrature hybrid.

The optical injection section of the OIPLL receiver, at the left of Figure 4, was constructed from fibre-pigtailed components. The lengths of the two paths from the input coupler to the inputs of the optical hybrid were matched to around 1 mm, despite the total length of each path being approximately 6 m. This ensured that the receiver could track variations in input signal frequency over a wide range. The receiver remained locked as a DFB laser used for the master signal had its temperature adjusted over more than 3°C, corresponding to a frequency change of more than 35 GHz (corresponding to a change in LO drive current of approximately 80 mA). For perfectly matched path lengths, the tracking range is in principle limited only by the continuous tuning range over which the LO laser delivers adequate power.

Differences in phase between the two paths due to thermal and other environmental changes were tracked by a control loop driving a fibre-stretcher phase shifter. The phase shifter was constructed by wrapping 10 turns of standard single mode optical fibre around a 40 mm diameter piezo-electric tube, giving a phase control range of more than 100π rad for a control voltage range of 150 V. All the optical components, including the slave laser, were placed inside a metal enclosure to shield them from air currents and to reduce the impact of temperature fluctuations.

Three polarisation controllers were required (labelled „PC' in Figure 4): two to match the polarisation of the signals at the inputs of the integrated optical hybrid to the polarisation-dependent fibres / waveguides of the hybrid (and therefore also ensuring that the master and slave signals are co-polarised when they are combined), and a third to align the polarisation of the injected signal with the field of the slave laser[*].

The slave (LO) laser was a three-section DBR laser controlled by an ILX LDC-3900 laser controller. Its temperature was controlled using a thermoelectric cooler. Tuning currents for the control loops were applied to the gain section of the laser via the modulation input of the laser controller. The bandwidth of the modulation input used was nominally 400 kHz. In some experiments, a second channel on the laser controller was used to bias the grating section of the laser to tune the laser wavelength. The phase control section of the laser was not biased. With just the gain section driven, the operating wavelength of the slave was approximately 1566 nm.

The scheme for controlling the fibre phase shifter is summarised here and described in more detail in Appendix 7.4. A 20 kHz sinusoidal dither current is applied to the slave laser gain section, thus modulating the free-running frequency of the laser. However, when the slave laser is injection locked to the input signal, this causes a dither in the locking phase, which is detected on the Q channel. We require the Q channel to act as a phase detector, so we wish to adjust the phase of the coherent mixing on the Q photodiodes so that the phase detector response is most linear (bringing the mean phase difference close to zero). This is done by minimising the magnitude of the second harmonic of the phase dither. This 40 kHz signal is detected using a lock-in amplifier in 2F mode, but since the signal is weak, an external notch filter is used to reduce interference from the fundamental at 20 kHz. The output of the lock-in amplifier drives the phase shifter through an integrator (time constant ~60 ms) to minimise static phase errors, and a high voltage driver amplifier. The overall gain of the path length control circuit was adjusted to give a response time of a few seconds. This is fast enough to track path-length variations due to temperature drifts, but slow enough to prevent interaction between this control circuit and the higher bandwidth PLL. Faster phase variations due to other environmental influences (e.g. vibrations) are tracked by the PLL.

Once the phase control loop is operating, and the Q channel is operating as a phase detector, the DC voltage at the Q channel output represents the locking phase of the optical injection locking, which reflects the free-running frequency offset between the master and slave lasers. The path through the loop filter can now be closed, in order to drive the voltage to zero and ensure that the slave laser tracks the master. The PLL loop filter is designed as a 2nd-order Type II PLL with a natural frequency of 1.5 MHz and a damping factor of 0.71 for a loop gain of 1.3 Grad/s/V[†]. However, the overall response of the OIPLL is dominated by the electronic feedback only at frequencies below a few kHz, with the optical injection locking dominating at higher frequencies.

[*] One of the polarisation controllers connected to the input coupler could be moved to the input side of the coupler to accommodate changes in the polarisation of the input signal more easily. Then, once initially aligned, the remaining two

[†] The loop gain is defined as the product of the gains of the loop components excluding the loop filter, i.e. the product of the phase detector gain and the slave laser tuning rate ("VCO" gain). The phase detector gain is determined by the responsivity of the quadrature channel detectors and the master and slave laser powers incident on them, and is typically 20 mV/rad. The slave laser tuning rate is approximately 0.5 GHz/mA which, when combined with the trans-conductance of the laser controller modulation input (20 mA/V), gives a VCO gain of 10 GHz/V.

The demodulated data is recovered from the output of the I channel by setting the phase shifter in that arm of the optical hybrid appropriately. This was done manually, although automatic control would be possible. The phase is adjusted by observing the output of the I channel on a spectrum analyser and then minimising the 20 kHz dither signal. The I and Q channels are then in quadrature. The fibre paths from the I channel outputs of the optical hybrid to the photo-receiver are matched to better than 2 mm (~10 ps), giving low distortion at 10 Gb/s.

3.2 Power adjustment

The receiver was typically operated with the mean signal power at the input set to +13 dBm by the erbium-doped fibre amplifier (EDFA) at the input. This power is quite large because of the excess loss in the data path, approximately 4 dB from the input of the receiver to the input of the optical hybrid and approximately 6 dB through the optical hybrid. Future improvements or alternative technologies may allow this excess loss to be significantly reduced. The output of the local oscillator (LO) laser was around +9 dBm, but allowing for loss in the circulator and the excess loss in the optical hybrid, the available power was less than +3 dBm, similar to the available signal power.

The control (Q) channel was set to give a phase detector gain of approximately 25 mV/rad at the output of the balanced detector, this being adequate to drive the control circuits without additional amplification. The splitting ratios of the input couplers in the optical hybrid were chosen in order to maximise the data eye amplitude while maintaining the required phase detector gain. Optical powers at the outputs of the hybrid under these conditions were -2 dBm (mean signal) and -1 dBm (LO) at the data (I) outputs, and -6 dBm (mean signal) and -7.5 dBm (LO) at the control (Q) outputs. These settings gave a data eye amplitude of around 230 mV from the amplified balanced detector (for coherently detected ASK data). Note that since the signal and LO powers on the data channel photodiodes are similar, the receiver is being operated with very low coherent gain.

3.3 Data-path optimisation

The RF amplifier in the balanced receiver was measured to have output thermal noise of standard deviation of 3 mV (measured using a 50 GHz digital communications analyser). With an eye amplitude of >200 mV the Q factor corresponding to thermal noise is therefore >30, which will give negligible penalty due to thermal noise (<0.2 dB OSNR penalty at a BER of 10^{-9}). It is this consideration which dictated the choice of optical powers described in Section 3.2.

Care must be taken to minimise patterning effects, particularly when using long PRBS patterns (e.g. 2^{31}-1). Best results were obtained by connecting the output of the balanced detector to the BER test set via as short a coaxial cable as possible (<50 cm) and a bias-tee (required for decision threshold adjustment) with a -3 dB bandwidth of more than 15 GHz. A patterning-limited Q of around 12 was estimated by the swept decision threshold method for this configuration for direct detection. This is calculated to give an OSNR penalty of <1.3 dB at a BER of 10^{-9} compared to ideal detection without patterning.

The actual configuration used for connecting the receiver to the measurement equipment differed in some of the experiments described in later sections. The impact of the electrical configuration is discussed where appropriate in those sections.

3.4 Noise-loaded transmitter

The transmitter consisted of either an external cavity tuneable laser or a standard DFB semiconductor laser, the output of which was modulated using a Mach-Zehnder modulator driven by

a 10 Gb/s pseudo-random NRZ electrical signal[‡]. By adjusting the bias point of the modulator, an optical signal with either binary amplitude shift keying (ASK) or binary phase shift keying (PSK) modulation formats could be generated (Figure 5). Since the coherent receiver gives an output signal proportional to the optical field (rather than the optical intensity, as is the case with direct detection), it is important to have a high extinction ratio in the case of ASK data to minimise eye closure due to residual light in 'zero' bits. The extinction ratio for ASK was typically 14 dB.

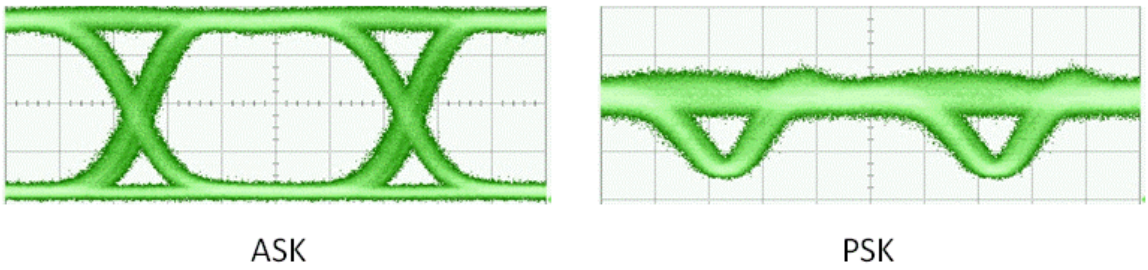

Figure 5: Transmitter optical eye diagrams for ASK and PSK modulation (10 Gb/s).

The OIPLL receiver was tested with variable input optical signal-to-noise ratio by noise loading the transmitter, using the arrangement shown in Figure 6. The output of the data modulator was combined with the output of a two-stage EDFA which acts as a source of amplified spontaneous emission (ASE) noise. The first EDFA stage was run at constant output power of around 0 dBm, while the output power of the second stage was varied. The output of the coupler was passed through a 1 nm optical bandpass filter to limit the total ASE power and then amplified to typically 13 dBm. The EDFA after the filter was operated with a relatively high input power (around -4 dBm), so with the noise loading EDFAs turned off, the OSNR at the output of the transmitter was high, greater than 40 dB / 0.1 nm. Using the arrangement shown, any combination of CW or modulated and noise-loaded or low-noise signals could be obtained.

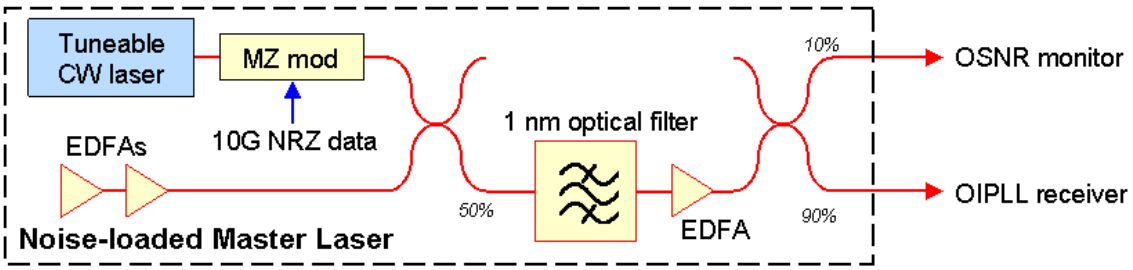

Figure 6: Noise-loaded transmitter.

A 10%/90% coupler before the receiver allowed the OSNR to be measured using an optical spectrum analyser. The OSNR was obtained by measuring the peak signal power and the noise power adjacent to the signal using an optical spectrum analyser set to a bandwidth of 0.1 nm. Corrections were applied to obtain the true signal power and the noise spectral density at the signal centre wavelength, taking into account variations in spectral density due to the optical filter shape or amplifier gain tilt. When making bit error ratio (BER) measurements, the output power of the EDFA at the receiver input was adjusted to keep the same peak signal power as the OSNR was varied, in order to ensure that the injection locking conditions and eye amplitude remain constant regardless of the noise level. The decision threshold was adjusted at each OSNR in order to minimise the BER.

[‡] Both lithium niobate and gallium arsenide Mach-Zehnder modulators were used during the course of the project.

4 RESULTS AND DISCUSSION

4.1 Phase noise measurements

The output of the balanced photodiodes on the Q channel represents the phase error between the master and slave lasers, and measurement of the noise spectrum at this point gives a great deal of valuable information about the phase tracking performance of the OIPLL (assuming the phase noise is larger than any amplitude noise). In practice, to avoid disturbing the PLL control loop and to take advantage of the integral RF amplifier, phase noise measurements were made from the data channel output, having first set the phase shift in that path of the optical hybrid to also give quadrature detection.

The noise spectrum was measured over several decades of frequency, and the recorded data combined and smoothed to give a spectrum on a logarithmic frequency scale. The spectra exhibit a strong peak at 20 kHz, corresponding to the dither applied to the slave laser, which modulates the locking phase of the optical injection locking (OIL). From measurements of the phase detector gain and the amplitude of the dither at the output of the Q channel, the variance of the 20 kHz phase dither can be calculated and used to calibrate the noise spectrum in rad^2.

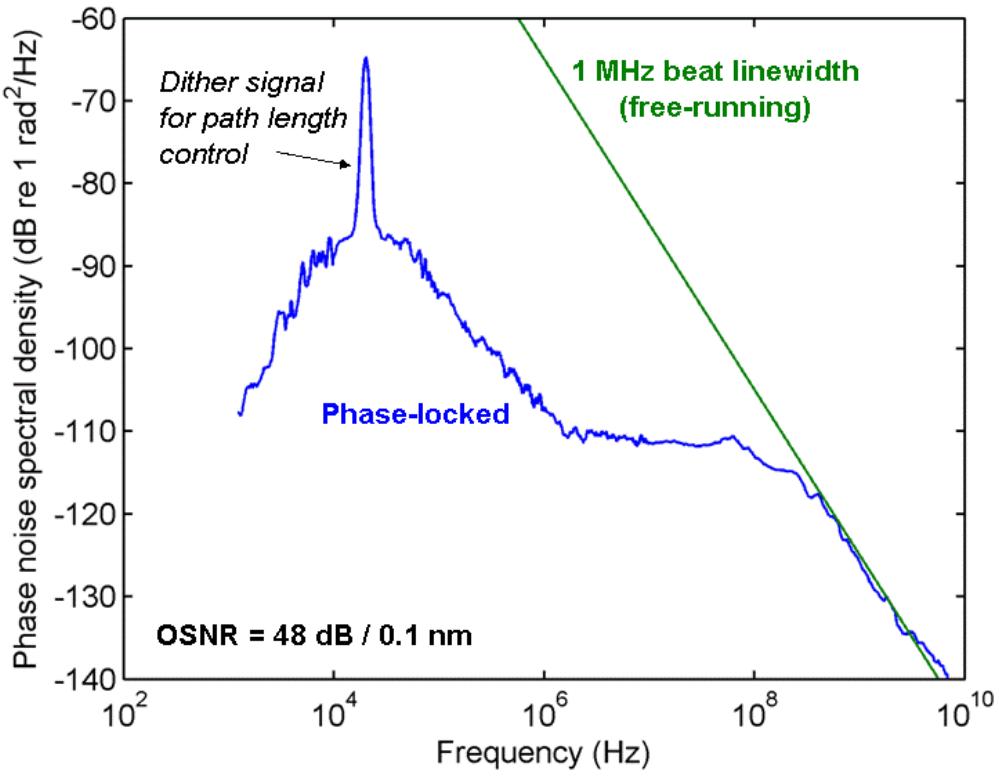

Figure 7: Phase noise spectrum for CW master signal.

The phase noise spectrum obtained in this way for a CW master signal with high OSNR is shown in Figure 7. The injection level was set to give a locking range of about 0.7 GHz. The strong dither signal at 20 kHz is clearly visible. Other features are interpreted as follows: At high frequencies (greater than a few hundred MHz), the spectrum rolls off as approximately $1/f^2$. This corresponds to the untracked laser phase noise outside the OIL locking bandwidth. In Figure 7, a line has been added to indicate the theoretical phase noise for a combined Lorentzian linewidth of 1 MHz, calculated from:

$$S_\phi = \frac{\Delta\nu}{\pi f^2}$$

where $\Delta\nu$ is the sum of the linewidths of the master and slave lasers and f is the frequency offset. This line coincides with the phase noise spectrum in the high-frequency region, indicating that the combined linewidth for the lasers used in the experiment is close to 1 MHz. At frequencies below a few hundred MHz, the measured phase noise is considerably lower than the theoretical spectrum, showing that the lasers are phase locked. Between approximately 1 MHz and 100 MHz, the phase noise spectrum is relatively flat at around -110 dB re 1 rad^2/Hz, but then increases at lower frequencies before rolling off below the dither peak at 20 kHz. This broad peak is believed to be caused mainly by noise on the laser current from the drive electronics, which is converted to phase noise in the same way as the applied current dither is converted into phase dither when the slave laser is locked to the master laser. The phase noise spectrum is shaped by the gain of the RF amplifier in the balanced photo-receiver, which rolls off below about 50 kHz.

The integral of the phase noise spectrum gives the phase error variance. In this report, values of the phase error variance are given for an integration bandwidth of 1 kHz to 10 GHz, and after subtraction of the contribution of the dither signal. For the spectrum shown in Figure 7, the phase error variance is found to be 0.003 rad^2. The phase error standard deviation is therefore 0.055 rad (3°), which is expected to have a very small impact on the BER of the demodulated data. By varying the master signal power injected into the slave laser, the locking range can be varied, which controls the phase tracking performance, as illustrated in Figure 8. The inset in Figure 8 shows that the phase error variance varies approximately in inverse proportion to the locking range, as expected from calculations based on a treatment of the optical injection locking as a first-order phase lock loop with a loop gain corresponding to half the locking range. For a locking range of 1.1 GHz, a phase error variance as low as 0.0017 rad^2 was obtained.

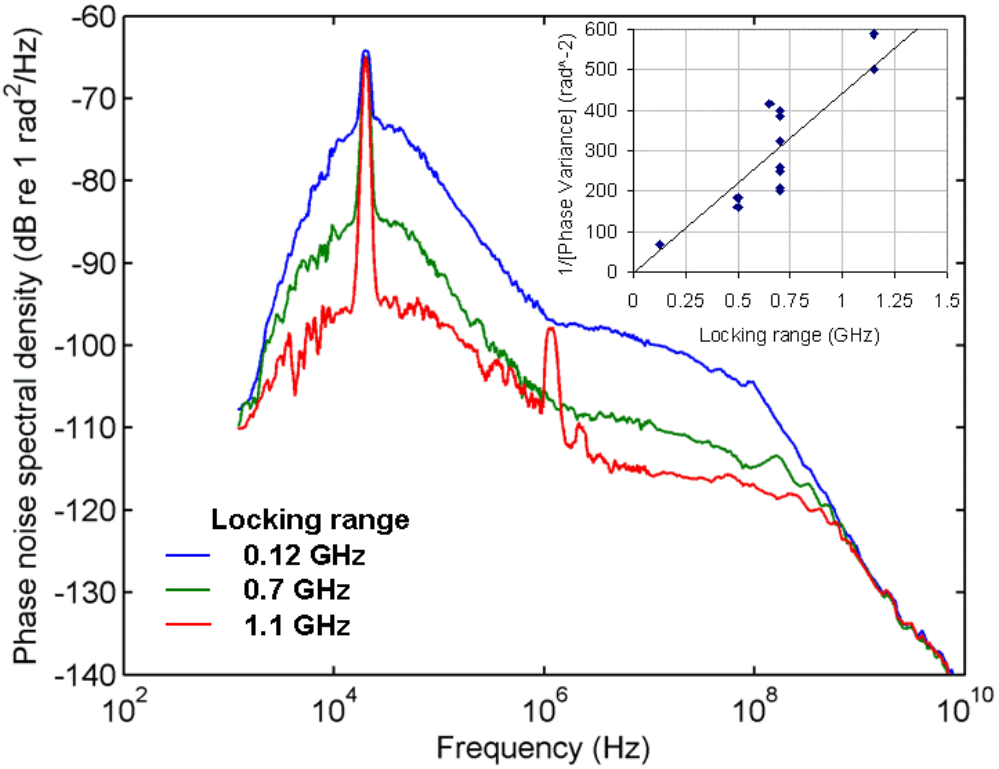

Figure 8: Phase noise spectra for various optical injection levels[§].

[§] In Figure 8, a peak is observed at approximately 1 MHz in the spectrum measured for 1.1 GHz locking range. This is due to a spurious signal generated by the ILX multi-channel laser current controller when the bandwidth modes of the channels are set in certain combinations. Similar spurious signals can also be observed in Figure 9 and Figure 10.

The impact of optical noise on the phase locking performance was investigated by noise loading the CW master signal. Phase noise spectra for different OSNRs are shown in Figure 9. For frequencies below about 10 MHz, the phase noise levels are unchanged, even for an OSNR as low as 10 dB / 0.1 nm. At high frequencies (above 1 GHz), the noise spectrum is dominated by amplitude noise due to beating between the slave laser and the ASE noise, not by phase noise. This was verified by measuring the spectra with the master laser turned off, but the added noise still present. A flat noise spectrum was observed from around 10 MHz upwards, at the same level observed in Figure 9 at around 10 GHz (below 10 MHz, noise from the receiver RF amplifier dominated). The phase noise translated slave-ASE beat noise is observed to vary approximately in inverse proportion to the OSNR, as expected from theory. Other amplitude noise contributions (master-ASE and ASE-ASE beat noise) are not observed as they are negligible compared to the slave-ASE beat noise. This is because they are reduced by the common mode rejection ratio of the balanced receiver, which is greater than 30 dB. One other feature in Figure 9 that is worthy of note is the peak in some of the spectra at about 70 MHz. The added noise appears to accentuate this feature, but closer examination revealed that both peaks and troughs in the spectrum can be observed at this frequency, even when no noise is added. It is thought that this feature is related to low-level reflections from the circulator, which affect the phase noise spectrum of the slave laser. The exact nature of the impact on the laser depends on the phase of the reflections, which fluctuates with environmental conditions. Overall, we conclude that optical noise at these OSNRs and power levels has little impact on the locking of the OIPLL receiver.

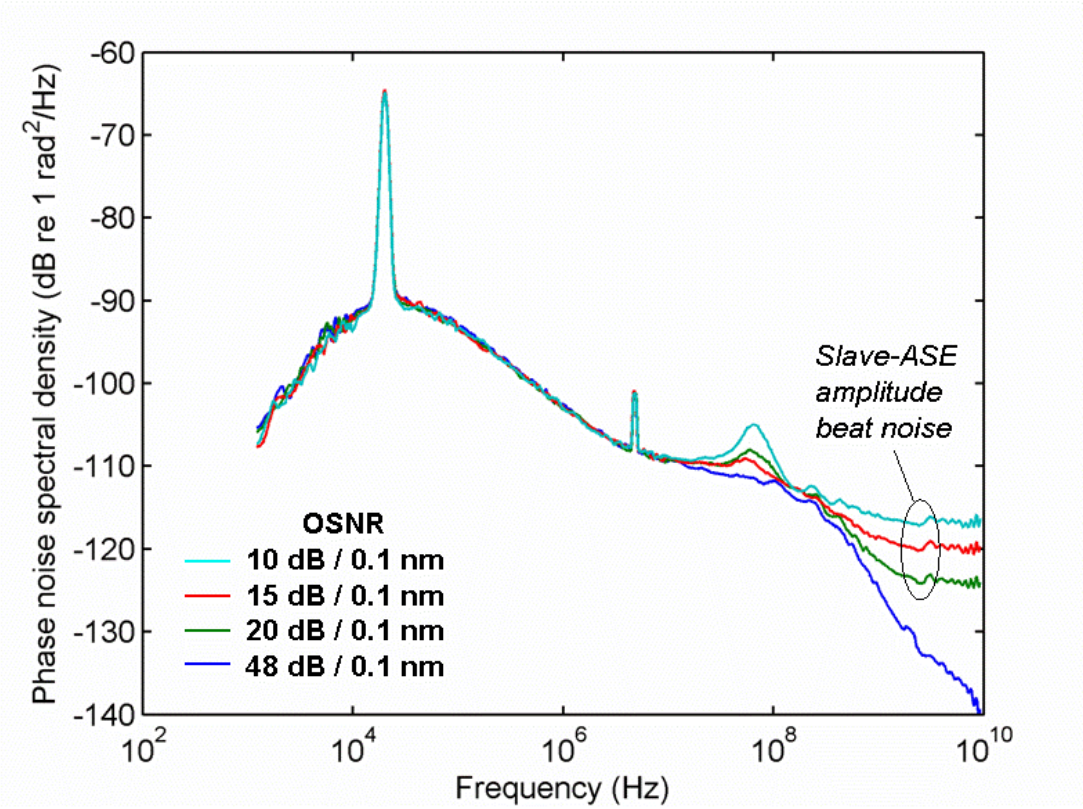

Figure 9: Phase noise spectra for noise-loaded CW master signal.

The phase noise spectrum was also investigated for a master signal modulated with 10 Gb/s ASK data. Figure 10 compares the phase noise spectra for CW and modulated master signals at high OSNR and for a modulated signal noise loaded to give an OSNR of 10 dB / 0.1 nm. The data pattern for the modulation was a 2^{31}-1 pseudo-random bit sequence (PRBS). At low frequencies (below about 10 MHz), there is little difference between the spectra, indicating that the receiver remains in lock even with data modulation and significant amounts of noise. The spectra differ at higher

frequencies (particularly above 100 MHz), but this is mainly because the modulation spectrum and the slave-ASE beat noise dominate in this frequency range.

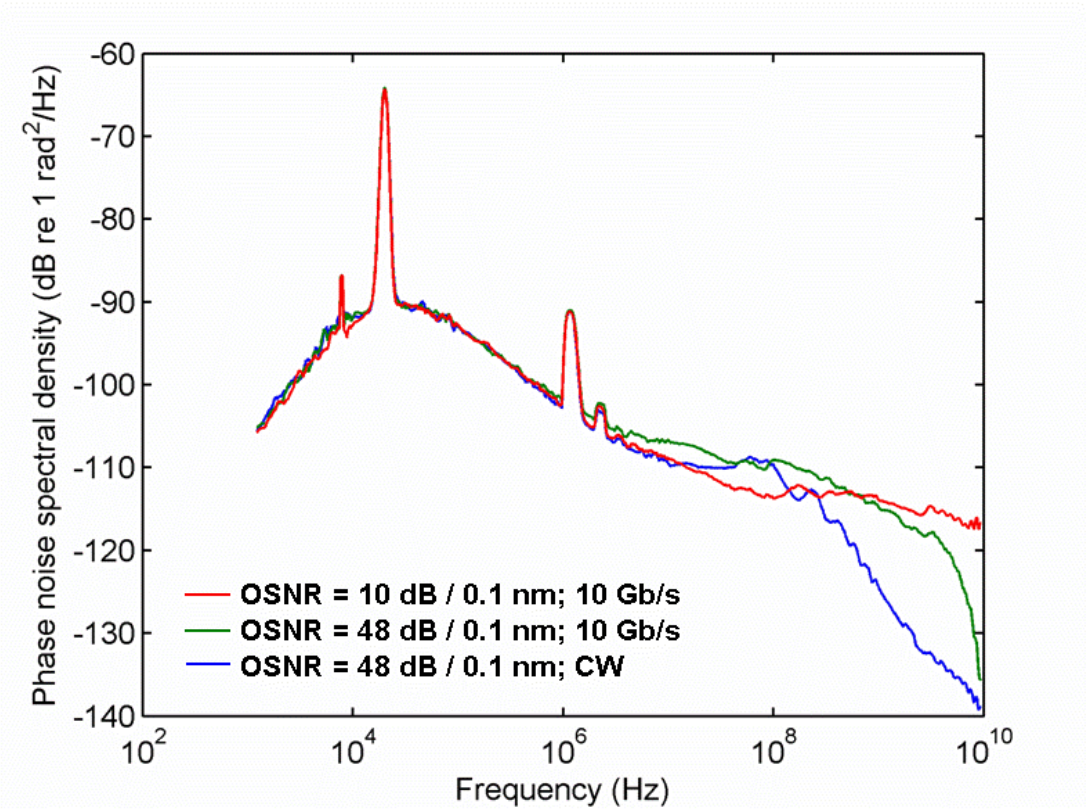

Figure 10: Phase noise spectrum with data modulated master signal.

4.2 Comparison with direct detection

Coherent homodyne detection of ASK data can theoretically give improved performance compared to IMDD in systems with optical amplifiers, by reducing the impact of ASE-ASE beat noise. To achieve this, the signal power must be much lower than the LO power (so that the noise is limited by LO-ASE beating), or balanced detection must be used to cancel the ASE-ASE and signal-ASE beat noise (see Appendix 7.1). For direct detection, the magnitude of the ASE-ASE beat noise depends on the optical bandwidth over which the ASE extends, so its impact is reduced by placing a narrow optical filter before the receiver. The improvement over direct detection achieved by coherent detection thus depends on the optical bandwidth and if ASE-ASE beat noise could be eliminated entirely (zero bandwidth filter), the theoretical performance of direct detection and LO-ASE limited coherent homodyne detection would be the same. Of course, the optical filter must not be so narrow that it distorts the signal, and manufacturing and alignment challenges dictate that practical filters are several times wider than the signal bandwidth. For 1 nm optical bandwidth, the OSNR required to achieve a given BER for 10 Gb/s ASK data is theoretically reduced by 1.5 – 2.5 dB with coherent detection (Appendix 7.3.3, Figure 30). Even if the optical bandwidth is reduced to 0.2 nm (25 GHz), coherent detection theoretically outperforms direct detection by around 1 dB.

To verify the expected improvement in performance with coherent detection, single channel measurements were carried out with a 1 nm filter placed before the receiver. Direct detection measurements were performed by turning off the LO laser and adjusting the data output coupler to give signal on just one of the photodiodes in the balanced detector. The input signal power was increased to give an eye amplitude similar to that for coherent detection. Since the optical hybrid is

polarisation sensitive, ASE in the orthogonal polarisation will be strongly attenuated, so the experimental results correspond to the theoretical calculation for one polarisation of ASE.

For coherent detection, the required OSNR for a BER of 10^{-9} was measured to be 15.8 dB (0.1 nm noise measurement bandwidth), while for a BER of 10^{-4} the required OSNR was 9.7 dB (Figure 11). The corresponding values for direct detection were 17.6 dB and 13.0 dB, giving performance improvements with coherent detection of 1.8 dB at a BER of 10^{-9} and 3.3 dB at a BER of 10^{-4}, in good agreement with the theory. The penalty for coherent detection compared to theory at a BER of 10^{-9} is around 1.2 dB, which is attributed to receiver patterning effects (see Section 3.3).

At BERs lower than 10^{-9}, the onset of an error floor was observed for coherent detection. With a short (2^7-1) PRBS no error floor was observed. The error floor is believed to be due to residual offsets in the free-running frequency difference between the signal and LO, as described in Section 4.7.3. The main source of the frequency offset is the dither applied to the LO laser, used to derive the control signal for the path length control loop. The error floor is therefore attributed to details of the current implementation, rather than fundamental causes. If, for instance, the receiver were implemented in integrated optics, active control of the path length would not be required, and the dither could be dispensed with.

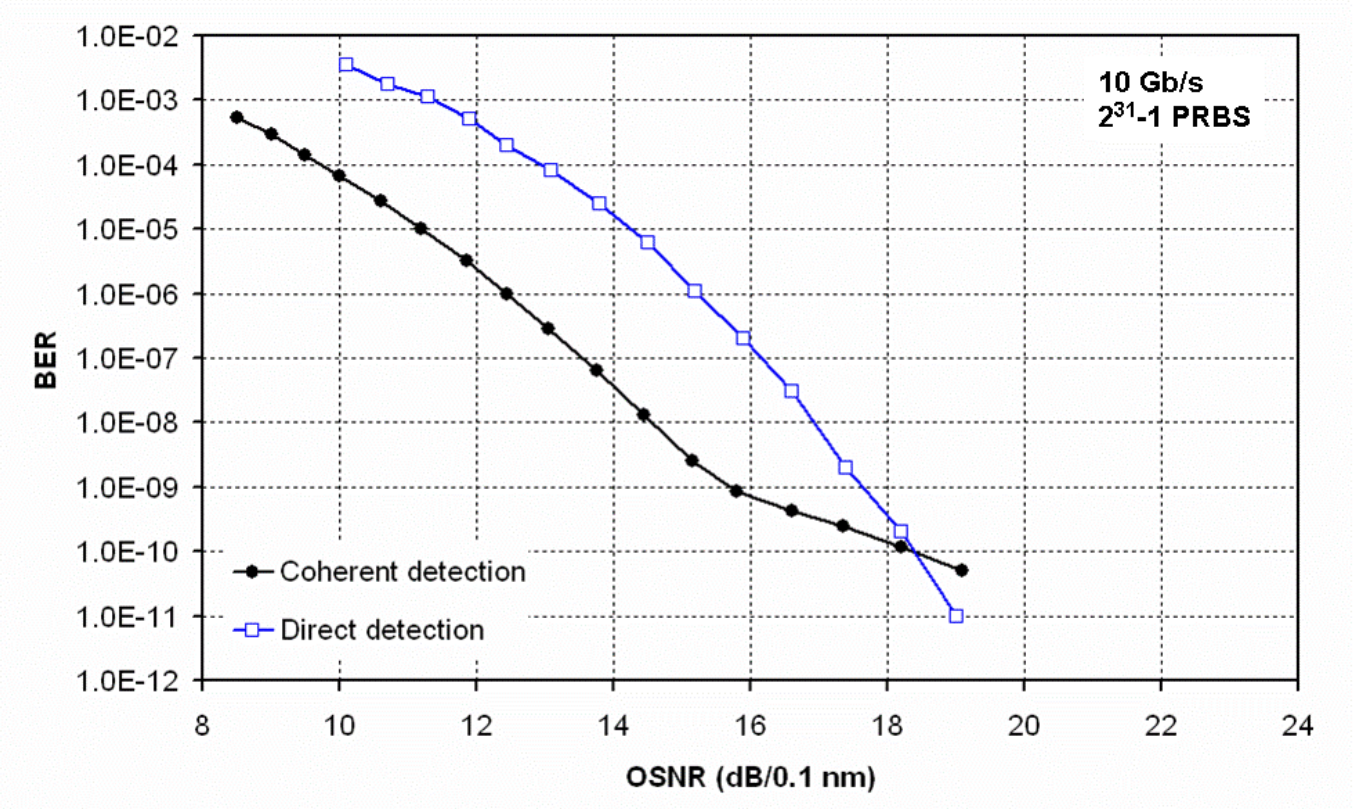

Figure 11: Experimental BER vs OSNR for coherent and direct detection of ASK data.

4.3 Channel selection with interfering channel

The high common-mode rejection ratio provided by the balanced detectors (≥25 dB) allows the coherent receiver to operate close to the LO-ASE limit even with a large input optical bandwidth, as illustrated in Figure 12, where BER vs OSNR measurements are compared for optical filter bandwidths of 1 nm and 5 nm[**]. In addition, directly detected components of the signal will also be

[**] The required OSNR for a given BER is larger for the results in Figure 12 than those in Figure 11 because the transmitter bias conditions had not been optimised when these measurements were made, and there was increased

suppressed, including those due to signals at other wavelengths. Provided the beat signal between the LO and adjacent WDM channels does not fall within the electrical bandwidth of the receiver, the coherent receiver can be used to select one channel from several WDM channels by tuning the LO laser to the wavelength of the wanted channel. These characteristics of coherent receivers offer an alternative to using a tuneable filter in conjunction with a direct detection receiver where a tuneable, frequency selective receiver is required, for instance in future agile optical networks, with the advantages that tuneable lasers are generally more readily available than tuneable optical filters and have higher tuning speeds.

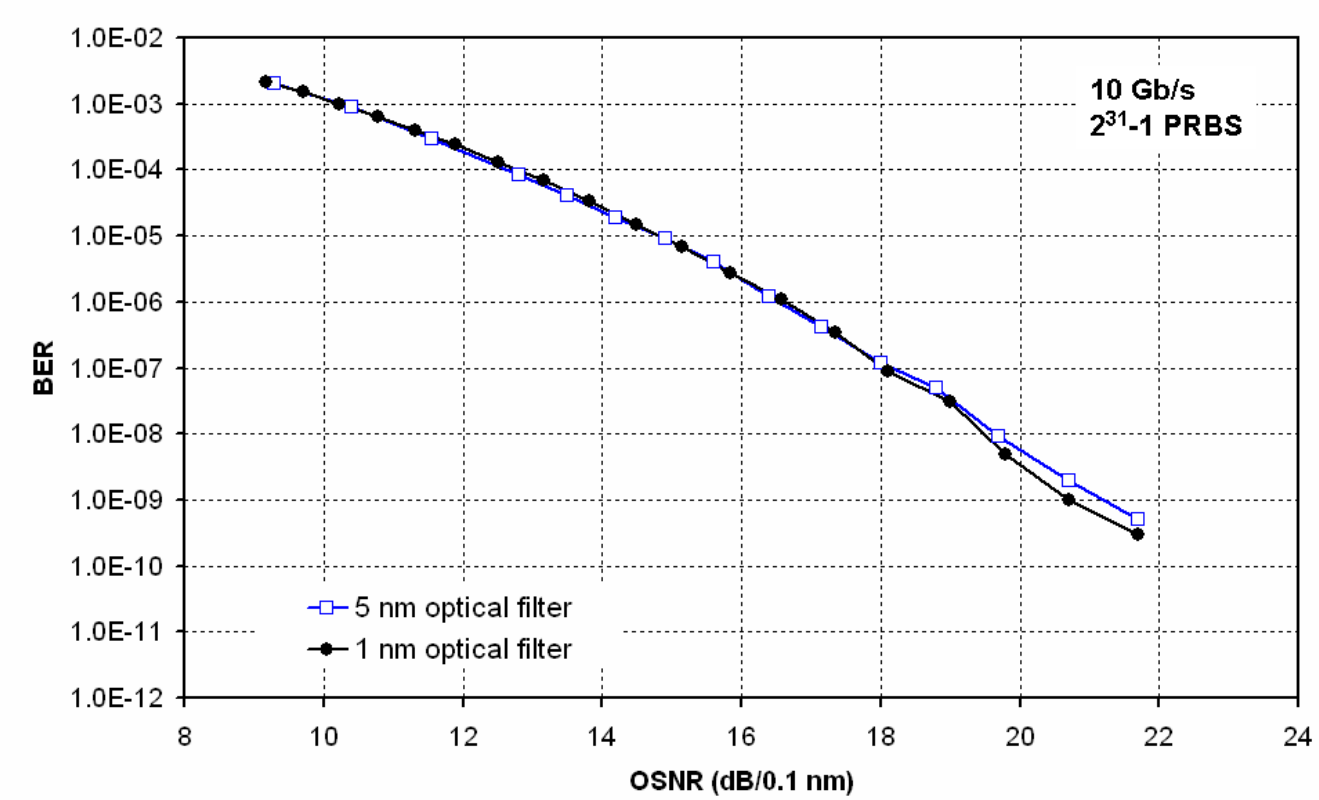

Figure 12: BER vs OSNR for coherent detection of ASK data with different optical filter widths at the receiver input.

To explore the operation of the OIPLL receiver in this frequency selective application, the experiment shown in Figure 13 was set up. The outputs of two external cavity tuneable lasers were ASK modulated by a 10 Gb/s 2^{31}-1 PRBS using Mach-Zehnder modulators and combined to form a two-channel WDM signal. One channel, at 1566.34 nm, was the „wanted' signal to be demultiplexed and demodulated by the coherent receiver, while the other channel provided an „interfering' signal at a variable wavelength offset. Electrical and optical delays between the two channels ensured that the data patterns were de-correlated and that bit transitions were not aligned temporally. The channels were adjusted to be co-polarised and to have equal power at the input of the receiver. The WDM signal was noise loaded with variable levels of ASE noise from two EDFAs and passed through a 5 nm optical filter.

receiver patterning due to a different electrical configuration being used after the OIPLL receiver (in particular, the bias-tee placed before the BER test set to adjust the decision threshold had a lower bandwidth [-3 dB at 10 GHz]).

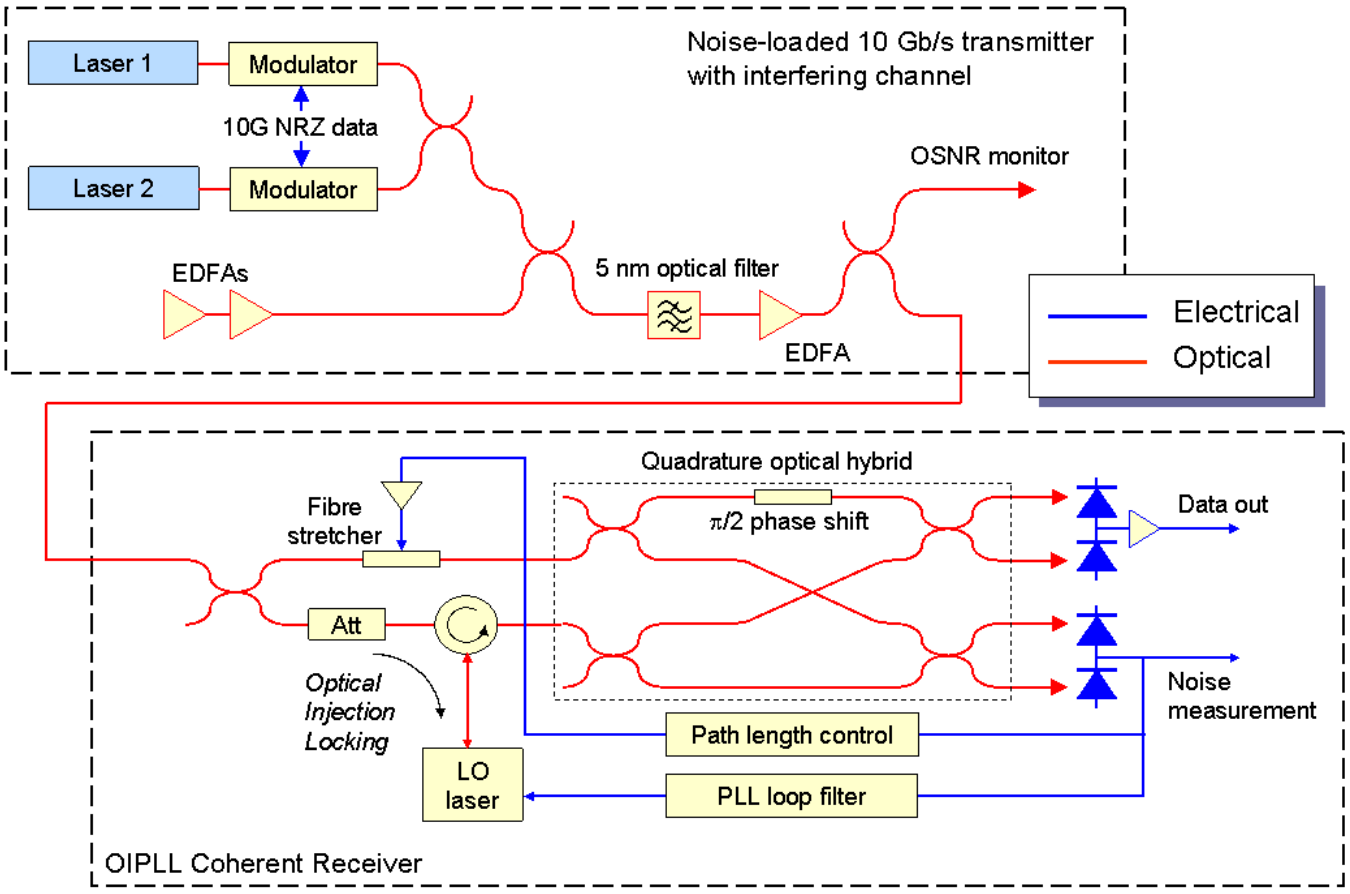

Figure 13: Experimental configuration for investigation of frequency selective operation of the OIPLL receiver.

BER measurements as a function of OSNR are shown in Figure 14 for demodulation of the wanted channel alone, and with the interfering channel at various channel separations. Operation with BER < 10^{-9} was achieved for channel separations of 25 GHz and 50 GHz, with a penalty of less than 2 dB compared to single channel operation. This penalty is thought to be due to the residual direct detection of the adjacent channel. For channel separations of 20 GHz and lower, an error floor was observed at high OSNR, due to beating between the LO and the adjacent channel signal falling within the electrical bandwidth of the receiver. The required OSNR for BER = 10^{-3} was approximately 10.5 dB for single channel operation and with channel separations of 50 GHz and 25 GHz. At a channel separation of 17.5 GHz, the OSNR penalty for BER = 10^{-3} was around 1.5 dB. These results suggest that demultiplexing of ultra-dense WDM channels should be possible if forward error correction techniques are applied.

A higher LO power at the photodiodes and / or lower receiver noise would allow the receiver to operate with a higher LO-to-signal power ratio, giving higher coherent gain. This would further suppress the direct detection components of the signal, giving lower penalty at wide channel separation and / or enabling rejection of more WDM channels. Optimisation of the electrical bandwidth of the receiver may give improved performance at narrow channel separation.

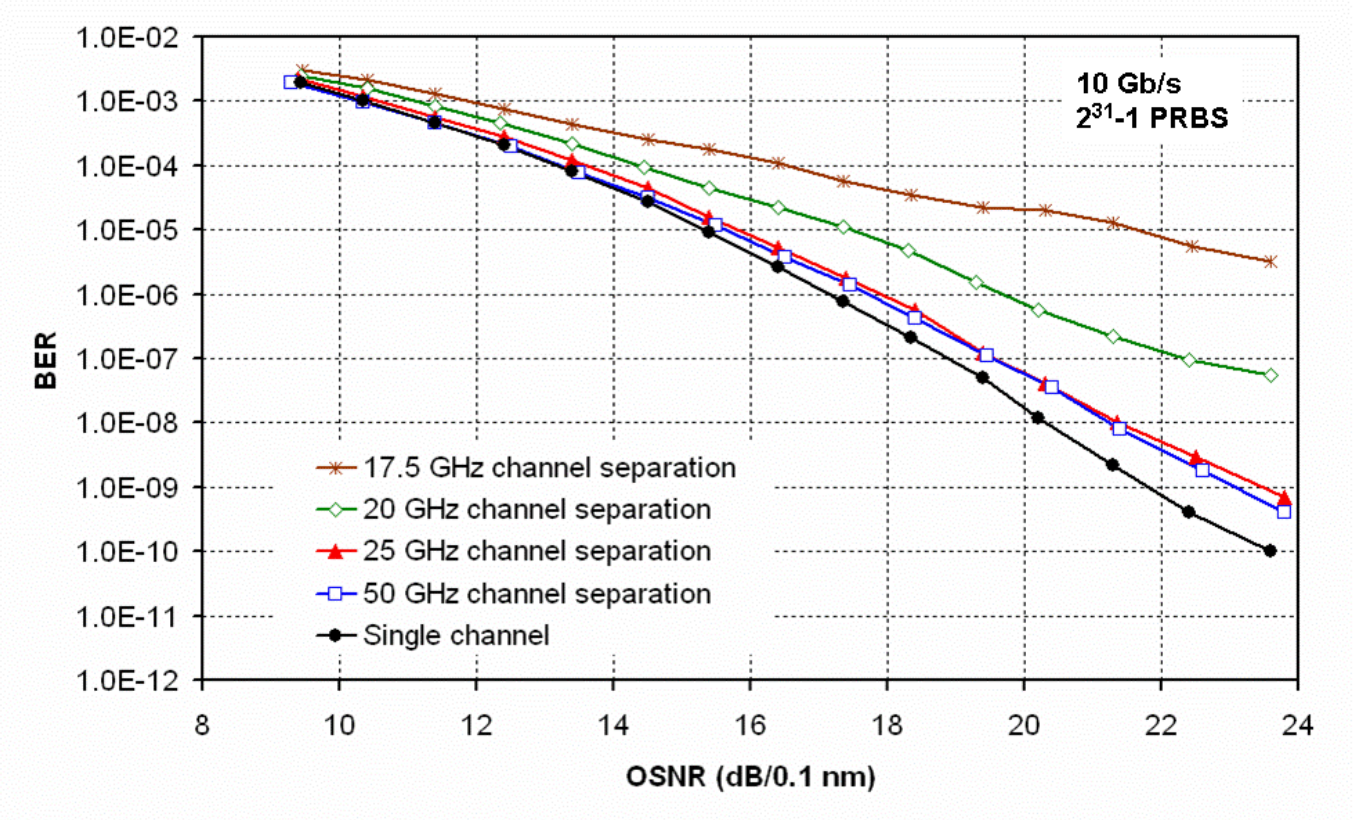

Figure 14: BER vs OSNR as frequency separation between wanted and interfering channels is varied.

4.4 Demodulation of dispersed signal

The measurements on the OIPLL receiver presented so far have all been for the back-to-back configuration, i.e. without transmission fibre between the transmitter and the receiver. An investigation of the tolerance to transmission impairments, in particular chromatic dispersion, is essential in order to evaluate the performance of any receiver in a real transmission system. The dispersion tolerance determines the maximum transmission distance without dispersion compensation, or the accuracy with which the dispersion must be compensated in a longer, compensated system.

As a starting point for an investigation of the dispersion tolerance of the OIPLL receiver, the BER vs OSNR has been measured for transmission over 40 km of uncompensated standard single-mode fibre (SSMF) with a total dispersion of approximately 700 ps/nm, using the experimental arrangement shown in Figure 15. In addition to the introduction of the fibre between transmitter and receiver, a polarisation tracker is placed before the OIPLL receiver to track variations in polarisation state at the output of the fibre, and a clock recovery unit is required to accommodate variations in transmission delay. Noise loading of the receiver is performed after the polarisation tracker, as we are interested in exploring the performance of the OIPLL receiver as the OSNR is varied, not that of the polarisation tracker as well. However, the penalty introduced by the polarisation tracker would also have to be considered in the case of a real system. The launch power into the fibre was chosen to be -1.5 dBm or lower, to ensure that any non-linear effects are negligible.

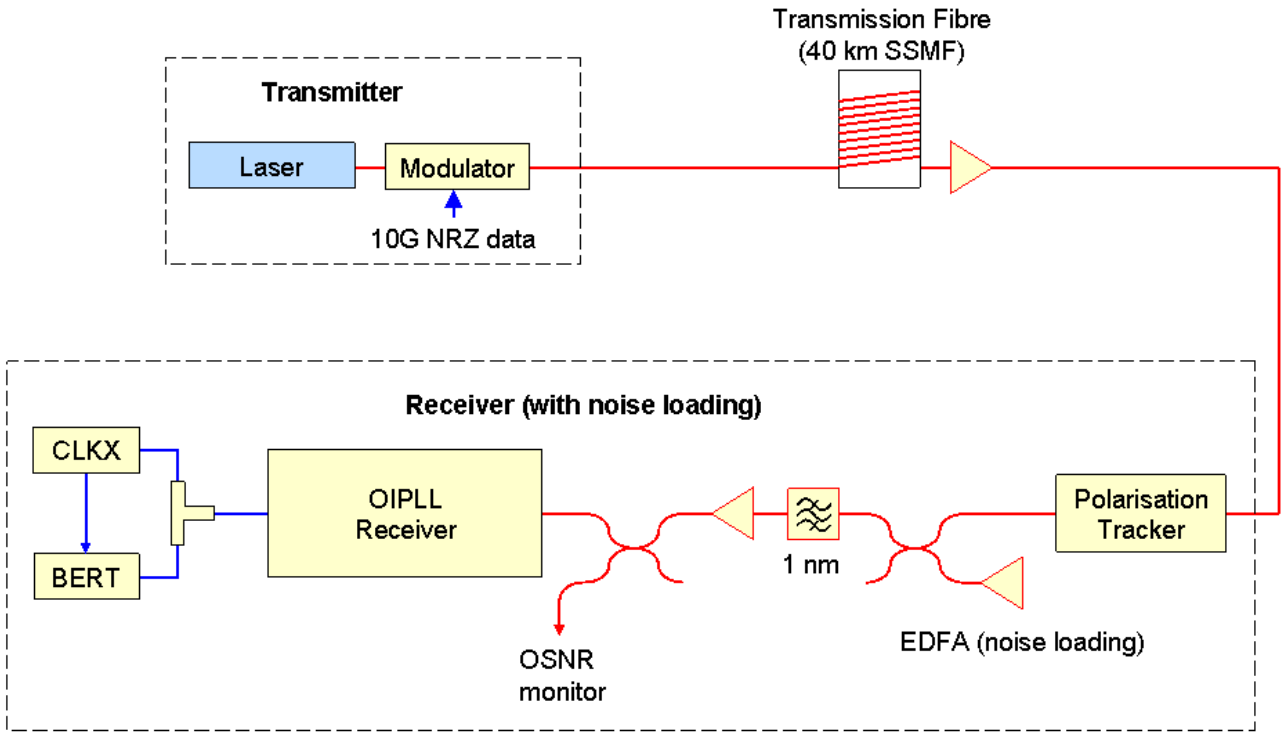

Figure 15: Configuration for fibre transmission experiment.

Preliminary results on transmission over fibre were presented in the report on Phase 3 of the project. These results showed an OSNR penalty compared to back-to-back operation of approximately 1 dB at a BER of 10^{-5} after 40 km of SSMF. However, the penalty increased at lower BER, with an error floor of slightly less than 10^{-9} being observed at high OSNR. A more detailed investigation of the system performance after 40 km of SSMF has been carried out as part of Phase 4, leading to the results presented here.

Despite attempts to improve the performance after transmission over 40 km fibre by making various modifications to the transmitter and receiver, the results obtained for a 2^{31}-1 PRBS were very similar to those obtained in Phase 3, with the BER after 40 km SSMF approaching an error floor of 10^{-9} at high OSNR (Figure 16). We conclude that this is simply because the limiting BER without fibre is quite high, as indicated by the error floor for the 0 km measurement at a BER of approximately 10^{-10} for OSNR greater than 18 dB. A relatively small eye closure due to dispersion is all that is required to increase the BER to around 10^{-9}. The relative eye opening can be estimated from the ratio of the Q factors corresponding to the limiting BERs. A BER of 10^{-10} corresponds to a Q of approximately 6.4, while 10^{-9} corresponds to a Q of 6, giving a relative eye opening of 94%. This is consistent with the eye observed after 40 km, which may be judged qualitatively to be „open'.

To further investigate the performance of the coherent transmission system over 40 km of SSMF, the measurements were repeated with a 2^{7}-1 PRBS. Much better performance was achieved at high OSNR, although an error floor was observed at a BER of around 10^{-11} (Q ~ 6.7) after the fibre.

At low OSNR, performance is limited by the LO-ASE noise, independent of the limiting BER at high OSNR. Similar measurements are obtained at a BER of 10^{-3} for the two PRBS lengths, with the OSNR penalty at this BER being 1.3 dB for 2^{7}-1 PRBS and 1.8 dB for 2^{31}-1 PRBS. The OSNR penalty due to LO-ASE noise alone can be shown to be equal to the square of the eye closure penalty (i.e. double the value in dB). Therefore this OSNR penalty corresponds to an eye closure of less than 1 dB, i.e. a relative eye opening of more than 80%. Again, this is consistent with the observed „open' eye, and in rough agreement with the earlier estimate of the eye opening.

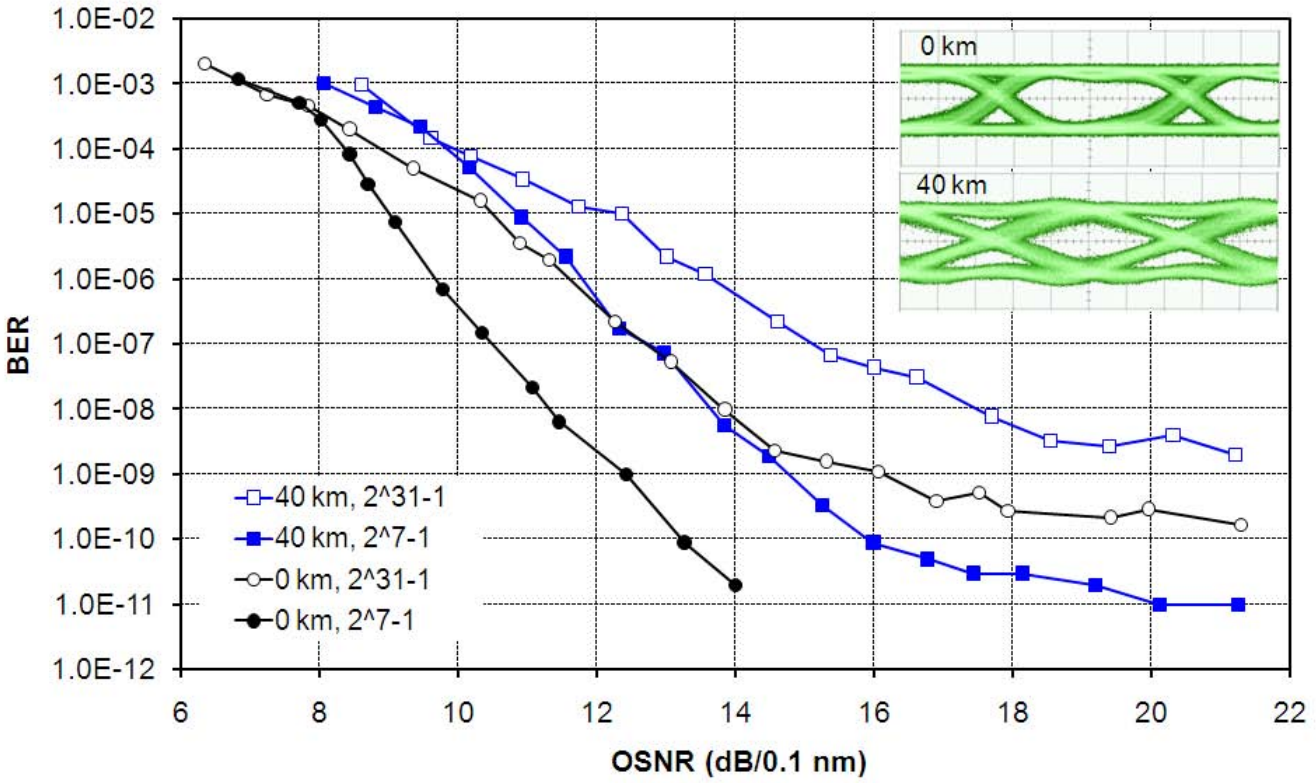

Figure 16: BER vs OSNR for coherent detection of ASK after 40 km of SSMF, compared to back-to-back performance (0 km). (The insets show the corresponding eyes, without noise loading.)

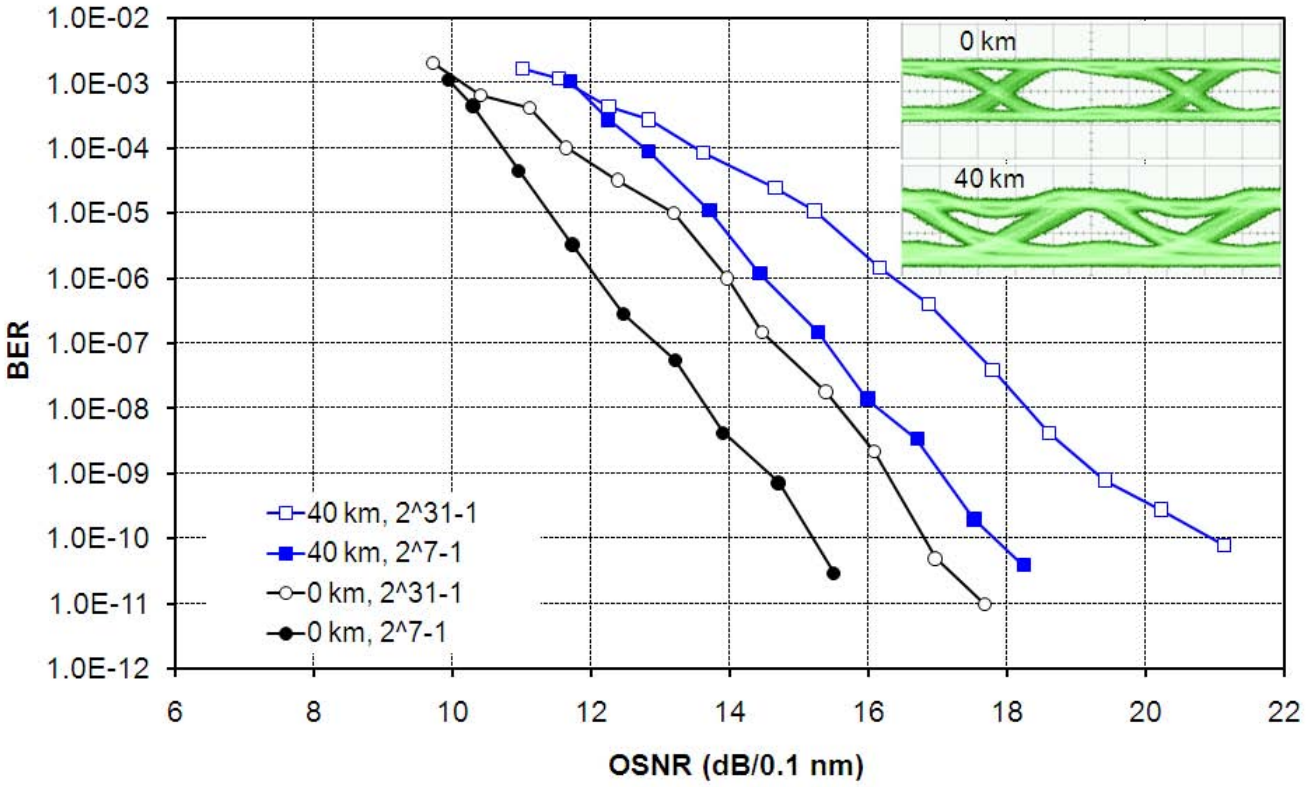

Figure 17: BER vs OSNR for direct detection of ASK after 40 km of SSMF, compared to back-to-back performance (0 km). (The insets show the corresponding eyes, without noise loading.)

For comparison, similar results for IMDD are given in Figure 17. At a BER of 10^{-3}, the OSNR penalty is 1.5 dB to 1.7 dB, corresponding to a relative eye opening of 84% and 82%, respectively. This is consistent with the 'open' eye observed for IMDD. The penalties due to chromatic dispersion over this length of SSMF (corresponding to dispersion of approximately 700 ps/nm) therefore appear to be similar for the two detection methods. However, for OSNRs less than about 18 dB, the coherent receiver outperforms direct detection over 40 km SSMF in terms of the required OSNR for a given BER. At high OSNR, direct detection gives the best performance, due to the absence of an error floor.

4.5 Locking to phase-modulated signals using orthogonal polarisation pilot

4.5.1 Data phase tracking by optical injection locking

Thus far, all the work described has focused on demodulation of binary ASK signals (equivalent to the intensity modulation used in direct-detection systems). Ideally, our carrier recovery / phase locking technique should be capable of operating with arbitrary signal modulation formats, particularly phase modulation formats such as binary or quaternary phase shift keying (BPSK or QPSK), or amplitude and phase modulation formats such as quadrature amplitude modulation (QAM), which are subjects of great research interest and likely to find widespread application in future commercial systems. Such modulation formats offer greater sensitivity / noise immunity (BPSK) or an increase in system capacity by transmitting two or more bits per symbol (QPSK or QAM).

In contrast to ASK modulation, these modulation formats have no carrier in their time averaged spectrum under ideal generation conditions, assuming a symmetrical distribution of symbol locations in the complex plane, as is usually employed. There is therefore no stable reference for a phase lock loop to track. Even if the signal generation is not perfect, resulting in some residual carrier in the time averaged spectrum, it will be at a low level, making locking harder. In addition, since the phase of the modulated signal is constantly changing, if we try to lock directly to signal, the phase lock loop will attempt to follow the phase of the signal, or at least that part of it that falls within its bandwidth. This problem can be overcome by using non-linear elements in the phase lock loop to re-generate a stable carrier to lock to. However, in the case of our scheme based on optical injection locking this is not practical.

The effect of the optical injection locking tracking the phase of the data signal is illustrated in the simulation result shown in Figure 18. The optical injection locking is modelled as a first-order phase lock loop, which has been shown to be a satisfactory model [2]. In this simulation, a low-level residual time-averaged carrier brings and maintains the average phase of the slave laser close to the mean value of the signal (0 rad). If the initial phase of the slave laser is not close to this value, pull-in can be relatively slow. However, the slave laser also tracks the varying signal phase, giving large phase variations correlated to the data, which would significantly degrade the demodulated signal. Reducing the bandwidth of the optical injection locking (by reducing the injection level) would reduce the phase error variance associated with the data tracking, but would also reduce the ability of the slave laser to track other phase errors, such as that associated with linewidth.

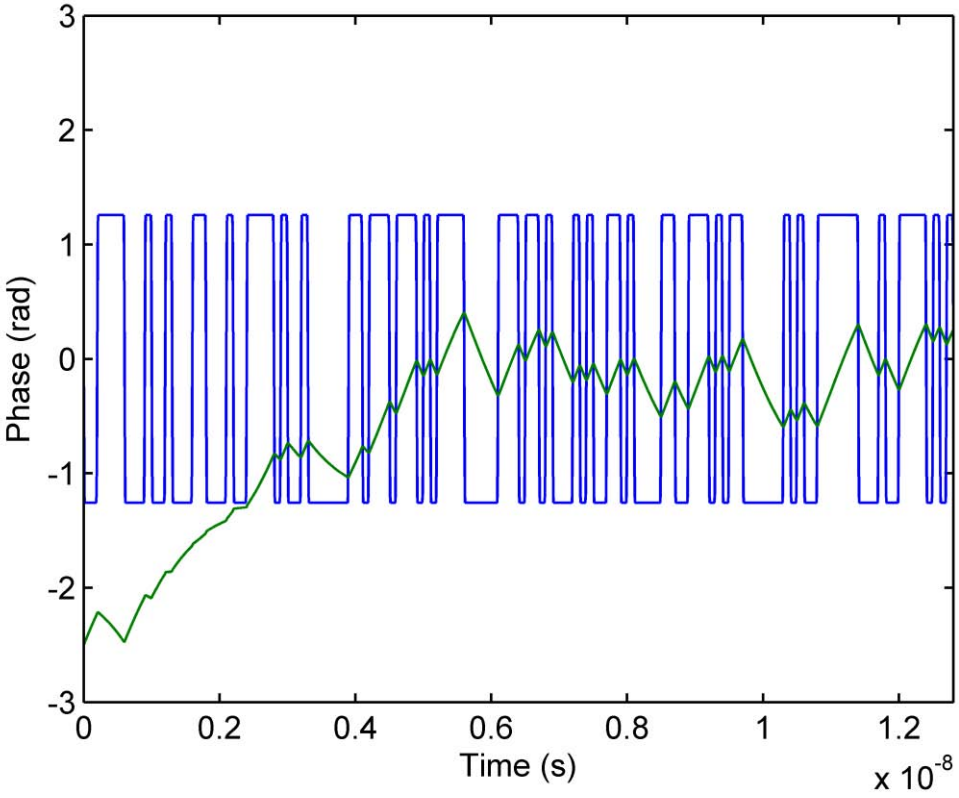

Figure 18: Simulated evolution of LO phase (green) for optical injection locking to a binary PSK signal with residual carrier (blue). The full locking bandwidth of the optical injection locking was 500 MHz.

To allow locking to these modulation formats with low phase error, an alternative approach is required. One possibility is to use a pilot tone at an offset wavelength [3]. However, this results in the signal being demodulated to an intermediate frequency. Wider bandwidth optoelectronic and electronic components are then required to detect and process the signal at the IF, and for high-bit-rate signals obtaining components with the necessary bandwidth is more difficult than for homodyne detection. In addition, the frequency offset between the signal and the pilot can introduce a penalty in the presence of PMD [4].

Here, we propose and investigate the use of an unmodulated pilot in the polarisation orthogonal to that of the data signal. This can be selected at the receiver and used to injection lock the LO laser. Provided the phase of the data is locked to that of the pilot at the transmitter (and remains locked), the LO can then be used to demodulate the data. Since only a low injected power is required to phase lock the LO, the power in the orthogonal polarisation pilot can be low, hence giving only a small penalty compared to direct locking.

4.5.2 Experimental arrangement

The signal with orthogonal polarisation pilot was generated using a GaAs Mach-Zehnder modulator which transmits both TE and TM polarised optical fields with low loss, but which only modulates the TE polarisation[††]. Thus by setting the input polarisation to the modulator to couple into both waveguide modes, a signal consisting of a combination of modulated TE polarisation and unmodulated TM polarisation (the orthogonal pilot) was obtained. The TE and TM waves therefore automatically have a fixed phase relationship (although, since the effective refractive index differs for

[††] Commercial modulators typically include polarisers to block the unmodulated polarisation, to ensure high polarisation extinction ratio. However, no polariser was fitted to the prototype modulator used in this work.

the two modes, there is a phase offset between them). The ratio of powers in the two polarisations can be set arbitrarily by varying the input polarisation to the modulator[‡‡].

The effect of introducing the orthogonal pilot is to reduce the extinction ratio of the optical signal, as illustrated in Figure 19. Since some of the power in the signal is not being used to carry information, there will be a penalty associated with the orthogonal pilot approach (c.f. the penalty introduced by a finite extinction ratio). However, this penalty can be kept small by making the power in the pilot much less than that in the modulated polarisation.

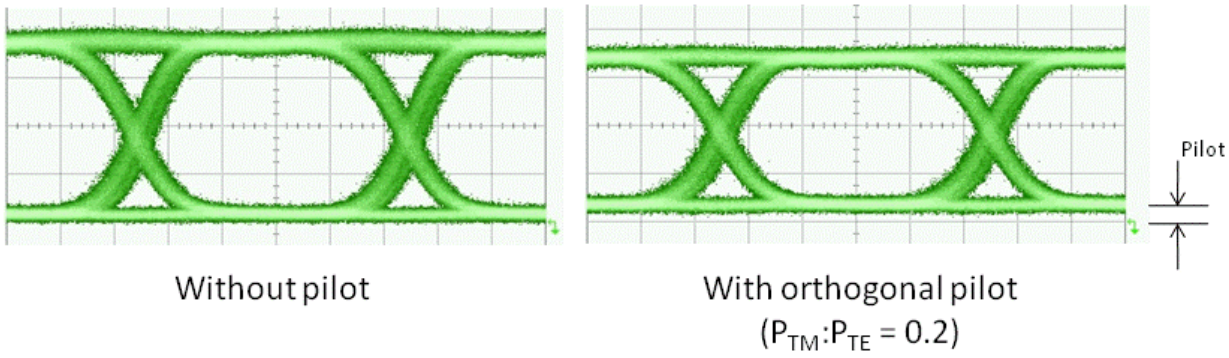

Figure 19: Transmitted optical ASK eyes with and without orthogonal polarisation pilot.

At the receiver, the polarisation controller on the optical injection locking path is set so that the pilot polarisation is aligned with the lasing polarisation of the local oscillator laser. The polarisation selectivity of the LO laser effectively filters out the modulated polarisation, and the LO laser injection locks to the unmodulated pilot. Since the power required for injection locking is very low, the pilot power can in principle also be very low[§§].

The polarisation of the signal at the input to the 90° optical hybrid was set to couple some of both modulated and pilot polarisations into the guided mode of the hybrid. In this way, the error from the "Q" channel contains a d.c. component from the pilot, enabling the low bandwidth feedback path to operate, and the demodulated data can be recovered from the "I" channel, after setting the phase shift in this arm appropriately. This introduces another penalty, but this was minimised by setting the polarisation so that the received eye amplitude was reduced by only a small amount[***].

For these experiments, a DFB laser was used as the signal laser.

4.5.3 Results

Measurements of back-to-back BER vs OSNR with locking to the orthogonal pilot are shown for binary ASK and PSK modulation formats in Figure 20. For these measurements the power in the orthogonal pilot was 20% of the mean power in the modulated polarisation (P_{TM}:P_{TE} = 0.2). The

[‡‡] Note that other ways of introducing the orthogonal polarisation pilot could be envisaged. For instance, some of the power from the transmitter laser could be tapped off before the modulator, and re-combined with the modulated signal through a polarisation beamsplitter after the modulator. However, in this case, it would be more difficult to maintain a fixed phase relationship between the two optical paths unless the splitter, combiner and modulator were all integrated into a single monolithic device.

[§§] If required, a polariser could be used to filter out the modulated polarisation before injecting the pilot signal into the LO laser.

[***] Schemes using appropriate polarisation filtering could be envisaged in which the phase error signal is derived solely from the pilot signal, while all the modulated power is directed to the data path.

result obtained for direct locking to ASK (i.e. without the orthogonal pilot) is also shown for comparison. In all cases a 2^{31}-1 PRBS was used at 10 Gb/s.

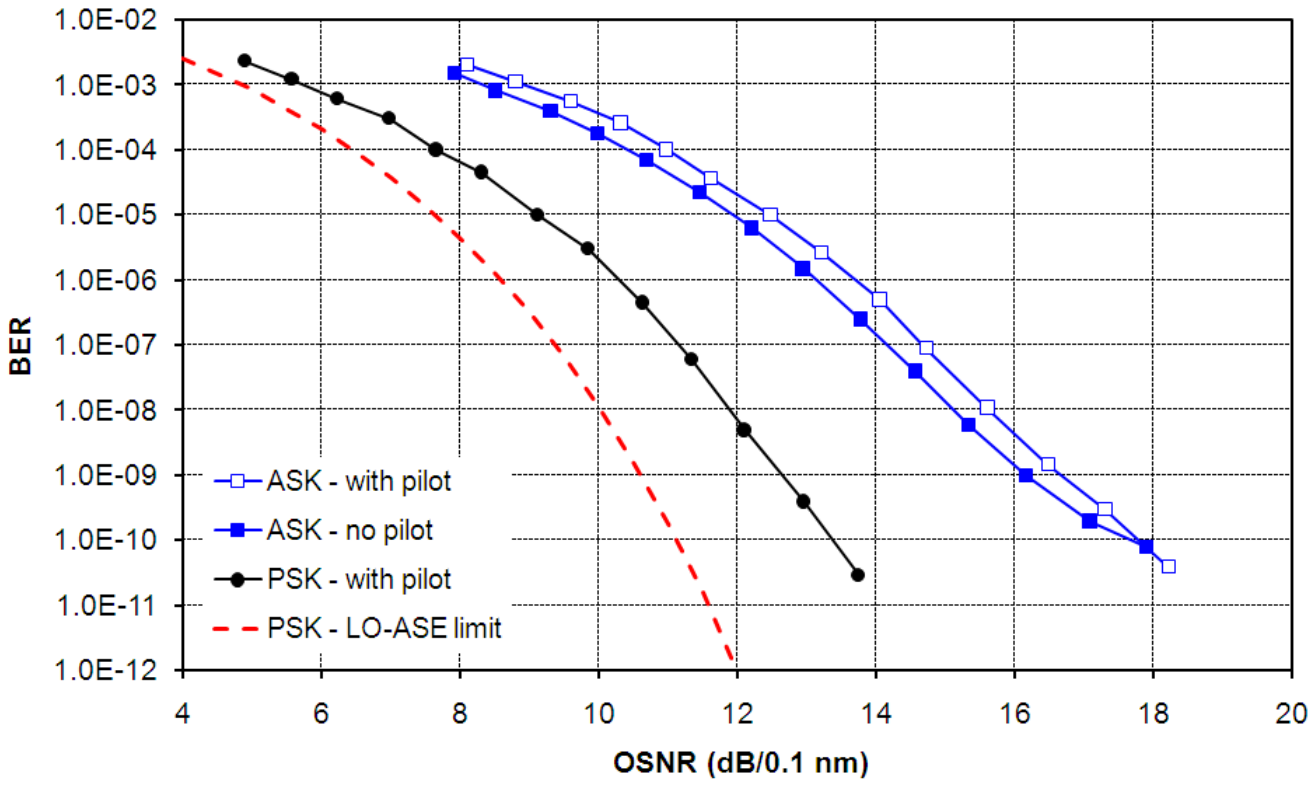

Figure 20: BER vs OSNR for detection of binary ASK and PSK signals using locking to orthogonal polarisation pilot. Experimental results for direct locking to ASK ("no pilot") and theoretical LO-ASE limit for PSK are included for comparison.

Looking first at the results for ASK, we observe that over most of the range of OSNRs explored, locking to the orthogonal pilot results in an OSNR penalty of approximately 0.5 dB compared to ASK with direct locking, due to the power lost to the orthogonal pilot. The penalty due to the power in the orthogonal pilot is $1+P_{TM}/P_{TE}$, giving a theoretical penalty of 0.79 dB compared to ideal ASK for $P_{TM}:P_{TE} = 0.2$. However, the ASK signal without pilot had an extinction ratio of 13 dB, resulting in a penalty of 0.43 dB compared to ideal ASK. Therefore, the penalty for using the orthogonal pilot compared to the experimental ASK without pilot is expected to be 0.36 dB. The small additional penalty observed is attributed to the misalignment of the signal polarisation to the hybrid input, required to generate a feedback control signal for the OIPLL.

At OSNR ≈ 18 dB (BER ≈ 10^{-10}), the results for ASK appear to cross. This is consistent with the error floor previously noted for direct locking to ASK. With locking to the pilot, the data suggest no sign of an error floor at these BER levels, and this was confirmed qualitatively by observing "error-free" operation at high OSNR (i.e. without noise loading). Subsequent measurements confirmed that with locking to the orthogonal pilot the error floor was significantly lowered: at high OSNR a BER of $1.5\text{x}10^{-13}$ was measured (14 errors in 150 minutes), compared to a BER of around $3\text{x}10^{-11}$ with direct locking.

Using locking to the orthogonal pilot, demodulation of binary PSK was achieved. This was not possible without the pilot. At a BER of 10^{-3}, where performance is limited by the OSNR, a reduction of required OSNR of 3.3 dB was obtained. This is in good agreement with the 3 dB expected from simple theory. At a BER of 10^{-9}, the reduction in required OSNR is around 4 dB. This is because the limiting BER at high OSNR is lower for PSK than for ASK, as all the limiting factors (phase error due

to linewidth and other causes, receiver thermal noise, patterning) affect the PSK signal less than the ASK signal (for the same signal power).

Also shown in Figure 20 is the theoretical performance for PSK, calculated assuming the only noise source is LO – ASE beat noise and that the receiver electrical noise bandwidth is 8 GHz. The experimental results differ from this curve by only 1 dB at BER = 10^{-3}, suggesting that all implementation penalties, including that for using the orthogonal pilot, are small.

Received electrical eyes for ASK and PSK with locking to the orthogonal polarisation pilot are shown in Figure 21.

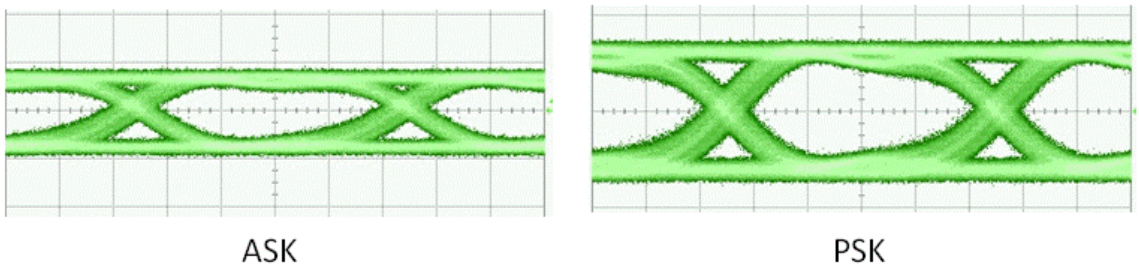

Figure 21: Received electrical eyes for binary ASK and PSK signals detected using locking to orthogonal polarisation pilot.

4.6 Impact of linewidth

To explore the impact of the combined linewidth of the transmitter and LO lasers, a DFB laser was used as the transmitter laser. By varying the drive current to the transmitter laser, the linewidth could be varied from less than 2 MHz to nearly 20 MHz (measured using the delayed self-heterodyne technique) – see Figure 22. The operating wavelength was kept constant (to match the wavelength of the LO laser) by adjusting the laser temperature as the current was varied. Optical amplifiers in the test arrangement ensured the power at the receiver remained constant.

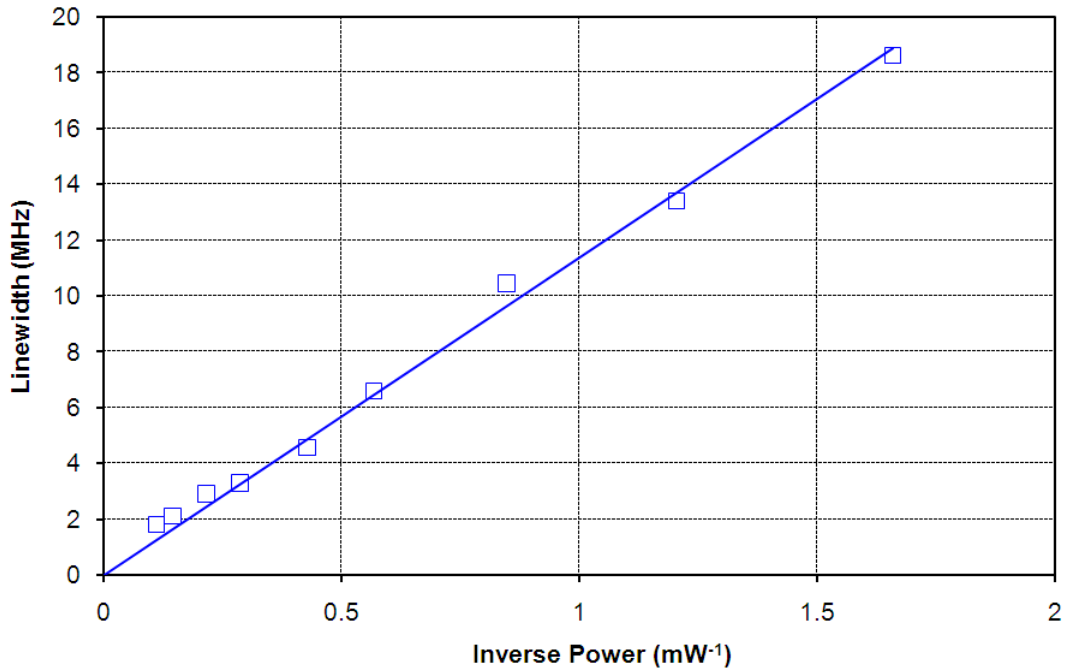

Figure 22: Linewidth of transmitter DFB laser.

The phase error variance for locking the LO laser of the OIPLL receiver to the CW transmitter laser was measured for each of these linewidths at an injection level which gave a full OIL locking bandwidth of approximately 600 MHz. At the LO laser drive current used, the LO laser linewidth measured using the delayed self-heterodyne technique was 1 MHz, close to that inferred from earlier phase error spectra using a narrow-linewidth transmitter laser.

Figure 23 shows the phase error variance (obtained by integrating the phase error spectrum over the frequency range 1 kHz – 10 GHz) plotted against the sum of the linewidths of the transmitter and LO lasers. The deviation from direct proportionality seen for summed linewidth less than 5 MHz might be due to non-Lorentzian contributions to the linewidth from intrinsic 1/f noise or noise on the laser current drive. These low frequency noise contributions can lead to the linewidth estimate obtained from the FWHM of the delayed self-heterodyne spectrum being greater than that of the Lorentzian component. However, the major contribution to the integrated phase error variance of the phase locked signals comes at large frequency offsets, where the contribution of the „tails' of the Lorentzian is dominant.

The BER was measured for the same linewidth conditions for ASK modulation using both 2^7-1 and 2^{31}-1 PRBS at 10 Gb/s and PSK using 2^7-1 PRBS at 10 Gb/s (Figure 24). Locking to an orthogonal polarisation pilot was used, enabling BER down to almost 10^{-13} to be achieved. Using the linear fit between phase error variance and linewidth shown in Figure 23, the BER data is re-plotted against phase error variance in Figure 25. In addition to the phase error due to the untracked linewidth, the dither signal applied for the path length control represents a small phase error. A fixed contribution to the phase error variance of 0.0025 rad^2 has been added to each point to account for this.

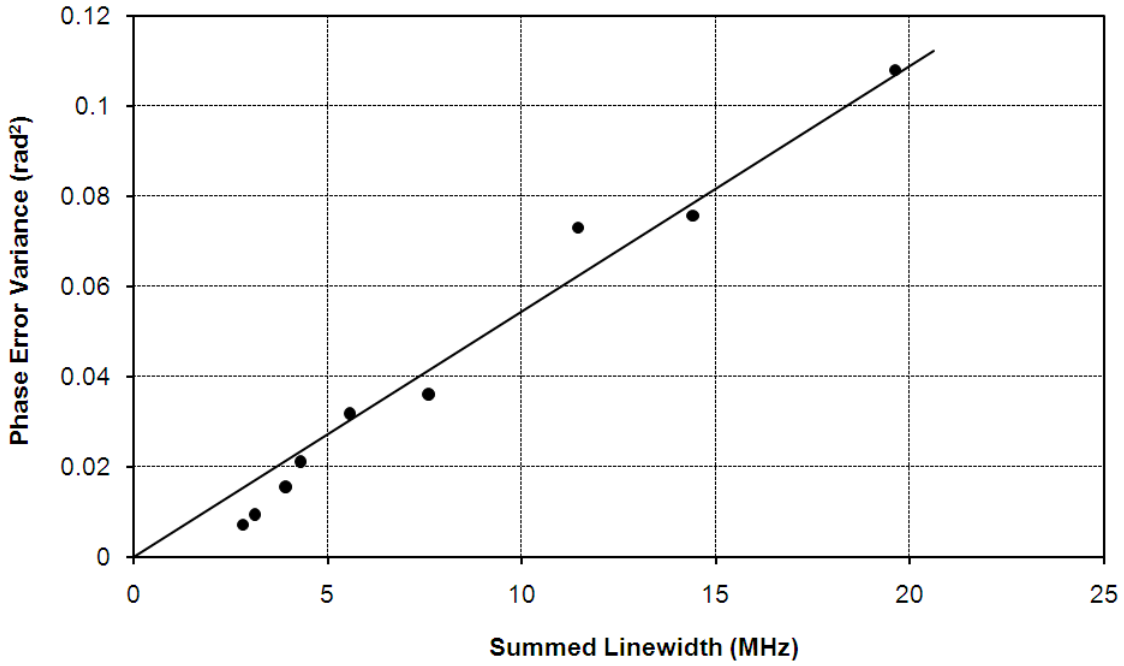

Figure 23: Phase error variance for CW locking vs the sum of transmitter and LO laser linewidths.

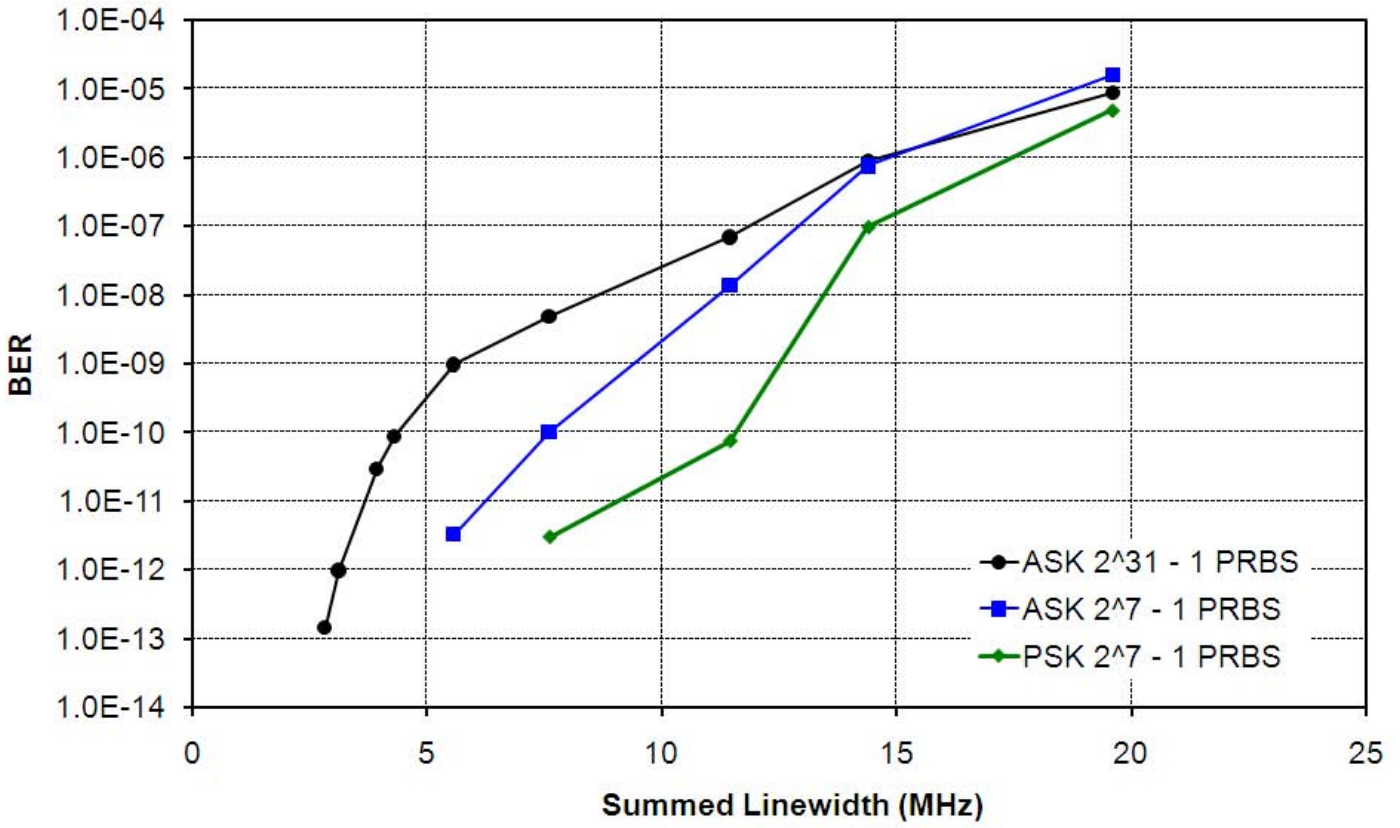

Figure 24: BER vs the sum of transmitter and LO laser linewidths for ASK and PSK signals.

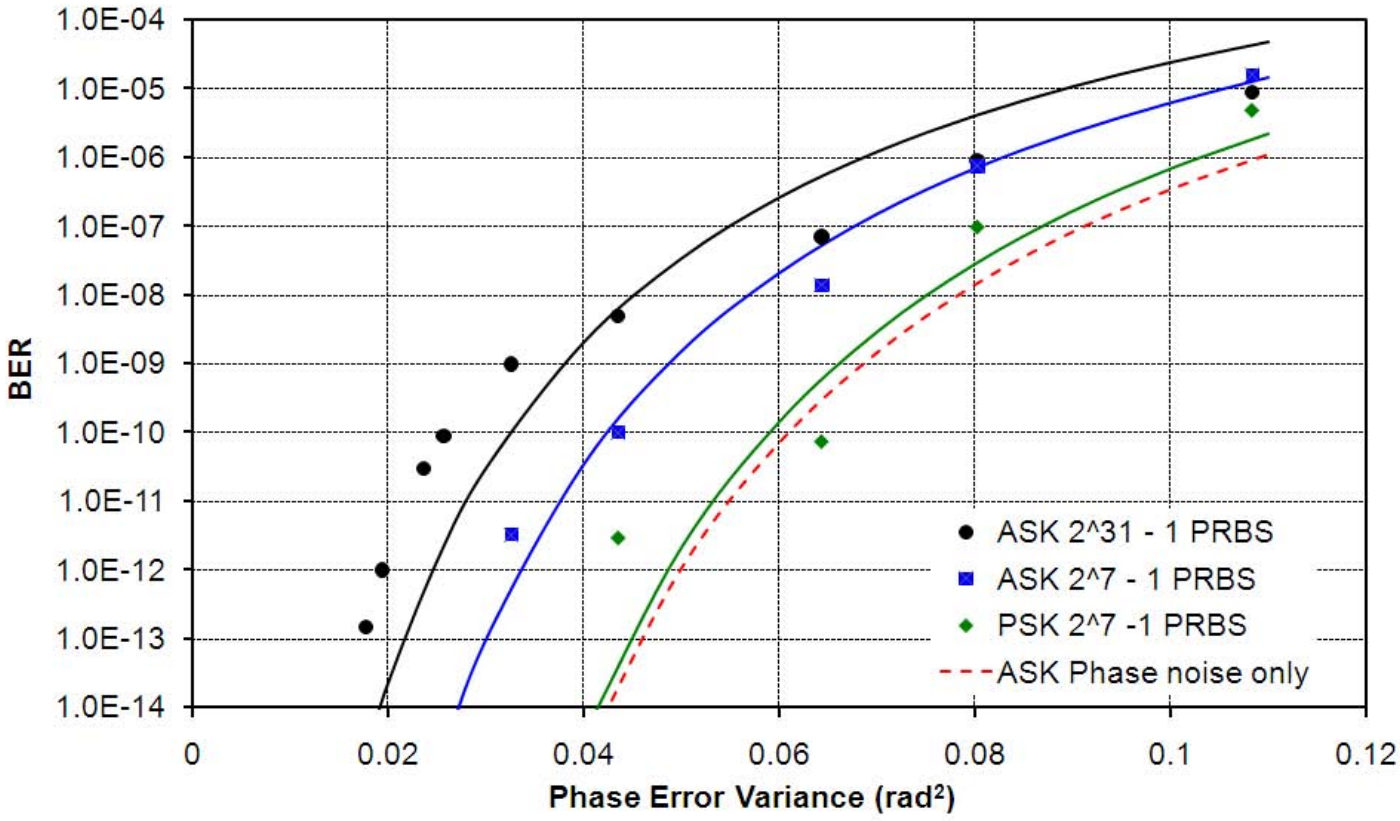

Figure 25: BER vs phase error variance.

The solid lines in Figure 25 are calculated values of the BER for the different conditions. For ASK, both phase noise and Gaussian amplitude noise (patterning and receiver thermal noise) must be taken into account. For a given phase error variance, the decision threshold level is selected to give the lowest overall BER, by balancing errors due to phase and amplitude noise. In the absence of phase noise, the BER is minimised by a threshold level close to the centre of the eye (assuming similar noise levels on the „ones' and 'zeros'). On the other hand, in the absence of amplitude noise, the BER due to phase error is minimised for ASK by setting the threshold close to the „zeros' level (giving the limiting performance shown by the broken curve). Therefore, when both noise sources are present, the BER is minimised by moving the threshold level closer to the 'zeros' level as the phase error variance is increased. To calculate the BER, the amplitude noise level was determined from estimates of the Q factor under conditions of low phase error variance. For 2^7-1 PRBS the value of Q used for the calculations was 13, while for 2^{31}-1 PRBS a value of 8 was used, reflecting the increased patterning with the longer bit sequence. Reasonable agreement is obtained between the experimental and calculated values.

For PSK, phase noise affects „ones' and „zeros' equally, so the optimum threshold level is at the centre of the eye for both amplitude and phase noise, and when both are present. For amplitude noise levels that give low BER rates, the BER for PSK should thus approach the theoretical minimum (twice the BER limit for ASK). For the measurements of PSK with 2^7-1 PRBS, the Q was estimated to be 16, so this condition applies. Reasonable agreement is again obtained between the measurements and the corresponding theoretical curve.

From Figure 25 we see that for BER less than 10^{-10}, the phase error variance should be less than 0.025 rad^2 in the more stringent case of a long PRBS. For the injection locking range used for these measurements, this corresponds to a combined linewidth of less than 4.3 MHz (Figure 24). For ASK with reduced patterning (2^7-1 PRBS) and PSK, significantly higher phase error variance and linewidth can be tolerated. For PSK, a phase variance as high as 0.06 rad^2 can be tolerated for a BER of 10^{-10}, corresponding to a combined linewidth of greater than 10 MHz for the injection locking conditions used in these experiments. These results therefore demonstrate that low BER operation is possible with the OIPLL receiver when lasers with linewidths of a few MHz each are used. The approach is therefore compatible with the semiconductor lasers typically used in commercial optical transmission systems.

4.7 Factors limiting performance at high OSNR

At low OSNR, the BER performance of the OIPLL receiver is dominated by ASE noise, and is found to be in good agreement with the theoretical limit imposed by LO–ASE beat noise. This results in improved performance with ASK modulation compared to direct detection. However, at high OSNR, the performance of the coherent receiver is affected by a number of factors which are not present for direct detection. In this section, these factors are identified and their impact summarised.

4.7.1 Receiver electrical noise and patterning

The minimum BER of all optical receivers is ultimately limited by receiver electrical noise, but this can be made negligible by increasing the signal amplitude. Then the receiver performance will be limited by patterning, where the amplitude of a single bit in the data stream depends on the sequence of bits that precedes it. For random data (approximated by a long PRBS), the amplitudes of the ensemble of „ones' or „zeros' will assume a distribution that is itself approximately random. This can result in errors in determining whether the received bits are „ones' or 'zeros', either directly due to patterning or due to a combination of patterning and noise. Since the coherent receiver detects the amplitude of the optical field, the effects of patterning may be different for coherent and direct detection. For instance, the distribution of levels in the 'zeros' of an ASK signal is broader in the coherently detected

signal than if the same signal is directly detected. This will result in a different optimum threshold point for the two detection methods.

Experimentally, the patterning limited Q factor was observed to be lower for coherent detection than for direct detection.

4.7.2 Dither phase error

The dither applied to the LO laser current as part of the path length control circuit results in a varying error in the locked phase. Measurements at large dither amplitudes show a similar variation in BER with phase error variance (due to the dither) as observed for varying the transmitter linewidth. Extrapolating to typical operating conditions where the lowest dither amplitude consistent with satisfactory operation of the control loop is applied, for which the phase error variance due to the dither is around 0.0025 rad^2, the BER limit due to the dither is estimated to be below 10^{-15}.

This source of phase error is related to the current implementation of the OIPLL receiver, and could in principle be eliminated (for instance, the path length control loop would not be required if the whole receiver were implemented in an integrated form).

4.7.3 Frequency error

For ideal ASK with an infinite extinction ratio, there is no power for injection locking during „zeros' in the data pattern. During this unlocked condition, any difference in the free-running frequencies of the transmitter and LO lasers will result in a linear increase in phase error. This does not result in errors in the 'zeros' (for zero signal power the coherently detected signal remains zero for all phases), but it can cause errors in subsequent „ones', as the phase does not recover immediately, but does so with a time constant related to the injection locking bandwidth, which is typically significantly less than that of the 10 Gb/s data signal. For ASK with a finite extinction ratio, the locking phase will differ for „ones' and „zeros' when there is a non-zero difference in free-running frequency, so there will still be a pattern-dependent variation in phase, although the excursion in long runs of „zeros' will not now increase without bound.

In the ideal case, the electronic feedback loop of the OIPLL should ensure that there is no difference in frequency between the lasers, so no phase error should build up during data 'zeros'. In practice, however, there are several potential sources of frequency error, including the dither applied for the path length control loop, offset voltages in the feedback circuit, and frequency jitter of the lasers outside the bandwidth of the electronic PLL.

This frequency error effect is believed to be the cause of the error floor at a BER of approximately 10^{-10} for direct locking to ASK data. From Figure 25, a BER of 10^{-10} corresponds to a phase error variance of around 0.025 rad^2 (for a 2^{31}-1 PRBS). Estimating the peak phase excursion as $\sqrt{2}$ times the r.m.s. phase variation, and assuming this builds up during the longest run of 'zeros' in the pattern (30 'zeros'), the maximum frequency offset is estimated to be approximately 12 MHz, similar to the frequency offset introduced by the LO dither for the path length control circuit, hence we can conclude that this is responsible for the majority of the phase error related to the frequency error effect. Note that although the dither is responsible for both the locked phase error described in the previous section and that due to the unlocked frequency error described in this section, the phase error variance due to the former is less than one tenth of that due to the latter.

Since this frequency error effect only occurs when the signal is zero (or too weak for effective locking), it is not present when the LO is locked to an orthogonal polarisation pilot (as described in Section 4.5). Hence it was possible to measure BER for ASK much lower than 10^{-10} in that configuration.

This source of phase error is related to the current implementation of the OIPLL receiver, and could in principle be eliminated (for instance, the path length control loop would not be required if the whole receiver were implemented in an integrated form).

4.7.4 Linewidth

The phase error associated with the untracked laser linewidth represents a fundamental limitation to the performance of synchronous coherent detection. However, with the optical injection level set to give a wide injection locking bandwidth, a linewidth related phase error variance of less than 0.002 rad^2 has been measured for an estimated combined linewidth of 1 MHz (see Section 4.1). In the absence of other sources of phase error (for instance, assuming an integrated implementation which does not require active control of the path length), this would be expected to result in an extremely small BER due to phase error ($<10^{-200}$), with BER limited in practice by patterning and receiver thermal noise.

5 FUTURE WORK

Two main potential developments of the current OIPLL receiver are envisaged, based on the results obtained in this project, as described in the following sections.

5.1 ASK receiver

With direct phase locking to ASK signals, the main benefits of the homodyne coherent OIPLL receiver are the lower required OSNR for a given BER compared with direct detection and the ability to select WDM signals without optical filtering (frequency selectivity). The lower required OSNR would allow system reach to be increased, while the frequency selectivity attribute might find application in broadcast-and-select or rapidly reconfigurable networks. However, these benefits would have to be weighed against the additional cost and complexity of the receiver and associated elements (e.g. polarisation tracking). Future development of the receiver should therefore consider how its cost might be reduced.

The first key step in any future development should be to make the receiver more robust and to reduce or eliminate the implementation-dependent sources of phase error that lead to the error floor at high OSNR in the existing implementation. This could be done by improving the path length control circuit to reduce the effect of the applied dither signal, perhaps by using more sophisticated phase-sensitive detection methods than those currently employed. Better still would be to eliminate the need for active path-length control, for instance by using an integrated optics approach for the whole receiver.

In terms of cost reduction, it should be noted that lower cost photodiodes could be used, rather than the high-speed balanced photodiodes used in the current implementation. A balanced detector is required for the electronic feedback path of the OIPLL, but this path only requires low-speed detectors, and this function could probably be implemented using two discrete photodiodes. Although the balanced detector on the data signal path provides excellent common-mode rejection, which is essential for frequency-selective operation, good rejection can be obtained with a single photodiode provided the ratio of signal to LO power is correctly chosen to give large coherent gain (LO power >> signal power) [5]. Limited LO power and high loss in the optical 90° hybrid prevent the current OIPLL receiver from operating in this regime, but by addressing these issues it may be possible to design a receiver with good frequency selectivity using a single high-speed photodiode on the data path.

5.2 IQ receiver

Using the technique of phase locking to an orthogonal polarisation pilot, detection of PSK signals has been demonstrated. The same technique could be used to detect complex modulation formats such as QPSK or QAM which allow more than one bit to be transmitted per symbol. This requires detection of the in-phase (“I”) and quadrature (“Q”) components of the signal on separate photodetectors. Assuming that the orthogonal pilot is phase aligned with neither the I nor Q components of the signal, we would therefore require a receiver with three detectors, for I, Q and feedback control. This adds complexity to the receiver, but, as noted above, low-speed detectors can be used on the control path, and single photodiodes could be used on the data paths, by making use of coherent gain. The comments in the previous section regarding improvement or elimination of the path-length control, and improving the robustness of the receiver also apply to the IQ receiver.

Other aspects of using the orthogonal pilot locking scheme requiring investigation before development of a full IQ receiver can be considered include how polarisation tracking would be implemented and controlled, and the impact of polarisation mode dispersion (PMD) in long fibre links, in particular the impact of its statistical variation with time, due to changes in environmental conditions, etc.

6 SUMMARY AND CONCLUSIONS

The concept, design, implementation and experimental evaluation of a novel homodyne coherent optical receiver are described. The receiver uses an Optical Injection Phase Lock Loop (OIPLL) for carrier recovery, which combines optical injection locking with low-bandwidth electronic feedback to give a low-delay, wide-bandwidth optical phase lock loop (OPLL) with large tracking range. The large effective loop bandwidth provided by the optical injection locking (typically around 1 GHz) far exceeds that obtainable with conventional OPLLs, enabling locking with very low phase error to be achieved, even with combined laser linewidths in the MHz region. The electronic feedback tracks low frequency noise, thermal drift of the injection-locked laser, and frequency drift of the incoming signal giving a robust system.

In the latest phase of the project (Phase 4), further experimental evaluation of the OIPLL receiver has been carried out, including a more detailed investigation of its operation following transmission of the signal over standard single mode optical fibre; demonstration of a modified phase locking scheme that allows detection of phase modulated signals; and a study of the impact of the transmitter linewidth on the receiver's performance.

Overall, through the course of the project, we have demonstrated the following key features and attributes of the OIPLL coherent receiver:

- Low BER operation at high OSNR for signal and local oscillator lasers with linewidths in the MHz range.
  - BER < 10^{-10} for 10 Gb/s binary ASK and PSK data.
- Performance close to the theoretical LO-ASE beat noise limit at low OSNR
  - Required OSNR ~6 dB/0.1 nm for 10 Gb/s BPSK, ~8 dB/0.1nm for 10 Gb/s ASK.
- Improved performance with ASK compared to direct detection
  - > 3 dB reduction in required OSNR at BER = 10^{-4} (1 nm optical bandwidth).
- Fibre dispersion OSNR penalty for binary ASK similar to direct detection
  - Less than 2 dB after 40 km SSMF.
- Frequency-selective operation due to high rejection of common mode signals (direct detection components and noise) as a result of balanced detection architecture
  - < 2 dB OSNR penalty at BER = 10^{-3} for 10 Gb/s ASK with equal power interfering channel 17.5 GHz from wanted channel.
- Large tracking range
  - > 35 GHz, limited in principle only by tuning range of LO laser.
- Very low linewidth-related phase error variance
  - < 2×10^{-3} rad^2 measured for 1 MHz combined signal and LO linewidth for CW locking (integration range 1 kHz to 10 GHz).

The main factors limiting the performance of the experimental OIPLL coherent receiver have been shown to be related to the current implementation using components with long fibre pigtails, requiring active control of the optical path lengths, which introduces additional phase errors. With suitable development, e.g. using an integrated optics approach, it should be possible to reduce or eliminate these implementation-related impairments. If this can be achieved, the very low linewidth-related phase error achievable would be expected to result in an extremely small BER (<10^{-200} for phase

noise variance of $2x10^{-3}$ rad^2), with the receiver performance then being limited in practice by patterning and noise.

7 APPENDICES

7.1 The effect of ASE beat noise on the OIPLL

Consider a signal from a master laser with added ASE noise, which is combined with the output of a local oscillator (slave laser) and detected using either a single photo-detector or a balanced photo-detector pair (Figure 26). The slave laser is locked to the master laser through an OIPLL arrangement, which is modelled by including the response of optical injection locking of the slave to the master in the loop filter, as well as the response of the electronic PLL filter [2]. The slave laser output is assumed to be a CW signal with no filtered ASE noise or residual modulation transferred from the injected noisy master laser signal. This is combined on the photo-detector with a portion of the unfiltered master signal plus ASE noise. For this analysis the master laser is assumed to be CW.

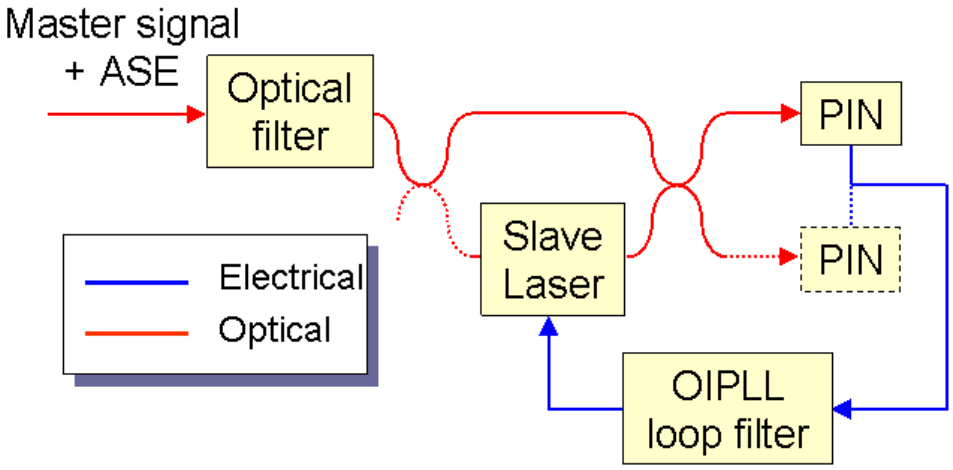

Figure 26: OIPLL configuration for noise analysis.

Assuming an homodyne OIPLL configuration, the electric fields at the two detectors ($E_{\pm}$) can be written in complex exponential representation as:

$$E_{\pm} = [E_m \mp jE_s \exp j\theta(t) + n_i + jn_q]\exp(j\omega_m t)$$

Equation 1

E_m and E_s are the amplitudes of the electric fields of the master and slave lasers respectively, and ω_m is the optical frequency of the master (and slave in this homodyne analysis). $\theta(t)$ represents the phase deviation between the master and slave lasers (the quiescent phase of the slave laser has been chosen to obtain the result in the conventional form for a PLL), and n_i and n_q are quadrature components of narrowband noise representing the ASE.

The detected signal is proportional to:

$$|E_{\pm}|^2 = E_m^2 + E_s^2 \pm 2E_m E_s \sin\theta + 2E_m n_i \pm 2E_s n_i \sin\theta \mp 2E_s n_q \cos\theta + n_i^2 + n_q^2$$

Equation 2

The first two terms are the directly detected master and slave laser signals, the third is the coherently detected signal, the next three are coherently detected noise (master-ASE and slave-ASE beat noise), while the last two are directly detected noise (ASE-ASE beat noise).

The detected current on each of the detectors can be written in terms of optical powers as:

$$i_{\pm}(t) = R(P_m + P_s \pm 2\sqrt{P_m P_s}\sin\theta + N_{m-ASE} \pm N_{s-ASE} + P_{ASE})$$

Equation 3

P_m and P_s are the master and slave signal powers incident on the photodetector, and R is the detector responsivity. P_{ASE} is the total ASE power in both polarisations, and the contribution of the polarisation orthogonal to E_m and E_s has been included in this expression. $N_{x\text{-}ASE}$ represents the master-ASE and slave-ASE beat noise.

For a locked loop, $\theta \approx 0$, so the noise terms in Equation 2 give:

$$i_{noise} \propto 2E_m n_i \mp 2E_s n_q + n_i^2 + n_q^2$$

Equation 4

For the case of balanced detectors, the overall current is:

$$i_b(t) = i_+ - i_- = R(4\sqrt{P_m P_s}\sin\theta + 2N_{s-ASE})$$

Equation 5

from which we note that only the slave-ASE beat noise remains.

The noise terms in Equation 4 may be identified as master-ASE, slave-ASE and ASE-ASE beat noises, for which the noise current variances are well known from the analysis of direct detection systems [6]. For the master-ASE and slave-ASE beat noise these are:

$$\sigma_{m-ASE}^2 = 2R^2 P_m P_{ASE}\frac{B_e}{B_o} \quad \text{and} \quad \sigma_{s-ASE}^2 = 2R^2 P_s P_{ASE}\frac{B_e}{B_o}$$

Equation 6

while the ASE-ASE beat noise variance for both polarisations is given by:

$$\sigma_{ASE-ASE}^2 = R^2 P_{ASE}^2 \frac{B_e}{B_o}\left(1 - \frac{B_e}{2B_o}\right)$$

Equation 7

B_o is the optical bandwidth (defined by the optical filter in the configuration of Figure 26) and B_e is the electrical bandwidth of the receiver.

In addition, there will be a shot noise contribution from each detector given by:

$$\sigma_{shot}^2 = 2eR(P_s + P_m + P_{ASE})B_e$$

Equation 8

Other amplitude noise sources (thermal noise in amplifiers, relative intensity noise of the lasers) are neglected in this analysis. The phase noise of the lasers (associated with the linewidth) will be included later.

Ignoring the DC terms (directly detected master and slave terms) and including the coherently and directly detected noise as a single term *N(t)*, Equation 3 may be re-written as:

$$i_+(t) = 2R\sqrt{P_m P_s}[\theta(t) + N'(t)]$$

Equation 9

where it has been assumed that $\theta(t)$ is small enough to allow linearisation. This corresponds to the standard expression used in PLL analysis for a linearised phase detector with added noise on one input [7]. $N'(t)$ is a phase noise equivalent, obtained by the translation:

$$N'(t) = \frac{N(t)}{2R\sqrt{P_m P_s}}$$

Equation 10

For balanced detection, the directly detected master and slave terms cancel, and the equation corresponding to Equation 9 is:

$$i_b(t) = 4R\sqrt{P_m P_s}[\theta(t) + N'(t)]$$

Equation 11

The phase noise spectral density for each of the noise components given in Equation 6 to Equation 8 is thus:

$$S_{N-x} = \frac{\sigma_x^2}{4R^2 P_m P_s B_e}$$

Equation 12

To see the effect of the detected noise, we must develop an expression for the OIPLL phase error spectrum that includes this contribution. Following Bordonalli *et al.* [2], we start from the basic (linearised) loop equation in the time domain:

$$\frac{d\phi_s}{dt} = k_{OIL}\theta(t) + k[\theta(t) + N'(t)] * f_{loop}(t) * \delta(t - T_d)$$

Equation 13

This describes how the slave laser phase (ϕ_s) is controlled by the slave laser frequency (time derivative of the phase) being adjusted by both the optical injection locking and the electronic loop in response to the phase error ($\theta(t)$). k_{OIL} and k are the loop gains for the optical injection locking and electronic phase lock loop, respectively; $f_{loop}(t)$ is the impulse response of the electronic loop; and T_d is the propagation delay of the electronic loop.

Taking the Laplace transform of Equation 13 we have:

$$s\phi_s(s) = k_{OIL}\theta(s) + kF_{loop}(s)[\theta(s) + N'(s)]\exp(-sT_d)$$

Equation 14

The phase error in the time domain is:

$$\theta(t) = \phi_m - \phi_s + \gamma_m(t) - \gamma_s(t)$$

Equation 15

where ϕ_m and ϕ_s are the quiescent phases of the master and slave signals, respectively, and γ_m and γ_s are their phase fluctuations. Differentiating, assuming ϕ_m does not vary, then taking the Laplace Transform and using Equation 14:

$$s\theta(s) = -k_{OIL}\theta(s) - kF_{loop}(s)[\theta(s) + N'(s)]\exp(-sT_d) + s[\Gamma_m(s) - \Gamma_s(s)]$$

Equation 16

Re-arranging to give $\theta(s)$ we obtain:

$$\theta(s) = \frac{s}{s + k_{OIL} + kF(s)\exp(-sT_d)}[\Gamma_m(s) - \Gamma_s(s)] - \frac{kF(s)\exp(-sT_d)}{s + k_{OIL} + kF(s)\exp(-sT_d)}N'(s)$$

Equation 17

or

$$\theta(s) = [1 - H_C(s)][\Gamma_m(s) - \Gamma_s(s)] - \frac{G_P(s)}{1 + G_I(s) + G_P(s)}N'(s)$$

Equation 18

where

$$G_I(s) = \frac{k_{OIL}}{s}$$
$$G_P(s) = \frac{kF(s)\exp(-sT_d)}{s}$$
$$G_C(s) = G_I(s) + G_P(s)$$
$$H_C(s) = \frac{G_C(s)}{1 + G_C(s)}$$

$G_I(s)$, $G_P(s)$, and $G_C(s)$ are the open-loop gains for the optical injection locking, the electronic loop and the overall OIPLL, respectively; $H_C(s)$ is the OIPLL transfer function.

The phase error spectrum for the OIPLL can thus be obtained as:

$$S_{OIPLL}(f) = [S_{PN-m}(f) + S_{PN-s}(f)]\left|1 - H(j2\pi f)\right|^2 + S_{N-tot}(f)\left|\frac{G_P(j2\pi f)}{1 + G_I(j2\pi f) + G_P(j2\pi f)}\right|^2$$

Equation 19

where $S_{N\text{-}tot}$ is the sum of the phase-translated spectral densities for the various noise components of the detected current, derived above. $S_{PN\text{-}m}$ and $S_{PN\text{-}s}$ are the phase noise spectral densities for the master and slave lasers respectively:

$$S_{PN-m}(f) = \frac{\Delta f_m}{2\pi f^2}, \qquad S_{PN-s}(f) = \frac{\Delta f_s}{2\pi f^2}$$

Equation 20

where Δf_m and Δf_s are the linewidths of the master and slave lasers respectively and Lorentzian line shapes are assumed. The phase noise variance is obtained by integrating Equation 19 over the range of frequencies of interest.

The first term in Equation 19 relates to the tracking of the phase noise (linewidth) of the master and slave lasers by the combination of optical injection locking and electronic feedback, and therefore depends on the transfer function of the whole loop (*H(f)*).

The second term in Equation 19 describes the effect of the noise on the detected current (mainly due to ASE noise), which is filtered by the electronic loop filter before being fed back to the slave laser. This noise is (incorrectly) interpreted as a phase noise to be tracked, and therefore adds to the overall phase noise of the OIPLL system. The transfer function in this term that filters the noise depends mainly on the response of the electronic loop.

Examples of phase error spectra calculated by this method are shown in Figure 27 for loop filter -3 dB bandwidths of 100 kHz and 10 MHz. A simple first-order low-pass filter response is assumed. An OSNR of 5 dB (with the noise measured in a bandwidth of 0.1 nm) and an optical bandwidth of 30 nm are used to accentuate the effect of the ASE noise. Other parameters used were:

Summed linewidth of master and slave lasers = 10 MHz
k_{OIL} = 4.2 Grad/s
k = 25 Grad/s
P_m = -10 dBm
P_s = 0 dBm
R = 0.62
B_e = 10 GHz (photodiode bandwidth)
Loop delay = 10 ns

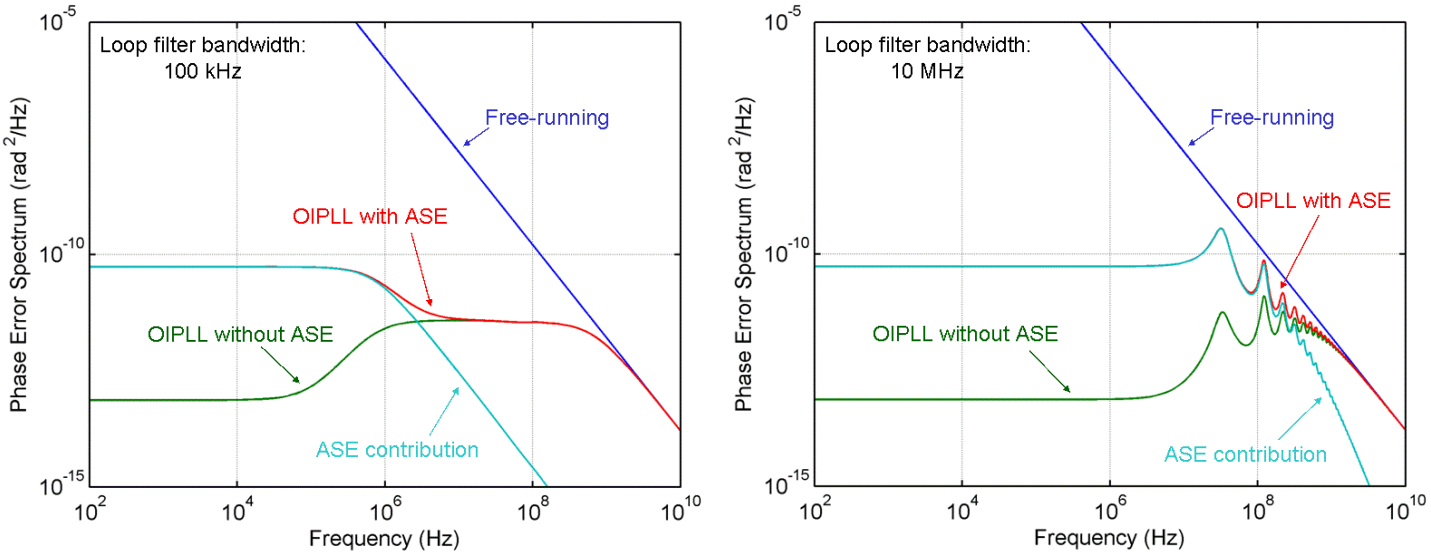

Figure 27: Example phase error spectra for OSNR = 5 dB / 0.1 nm and optical bandwidth = 30 nm.

The oscillatory behaviour in the spectrum for a loop filter bandwidth of 10 MHz is due to the non-zero loop propagation delay assumed.

For the same parameters, but varying the OSNR and loop filter bandwidth, the phase error variance is plotted in Figure 28. Under these conditions, at low OSNR the phase error variance increases due

to the effect of the ASE beat noises. However, a low phase error variance (<0.05 rad^2) is maintained to low OSNRs, even for the assumed optical bandwidth of 30 nm and a loop filter with a -3 dB bandwidth of 10 MHz.

If the electronic loop bandwidth is very small (around a kilohertz, say, as in our experimental OIPLL), then the contribution of the ASE noise to the overall phase noise can be expected to be completely negligible, even at very low OSNR. However, as reported in detail in the report on Phase 1 of the Project, the ASE has another effect, namely to broaden the linewidth of the slave laser, leading to an increase in the phase error variance. This effect can be minimised by reducing the injected ASE noise power, which can be done by reducing the master power or by using narrower optical pre-filtering. Since in the homodyne OIPLL the injected master power is very low (< -30 dBm), the injected ASE causes negligible broadening in this configuration.

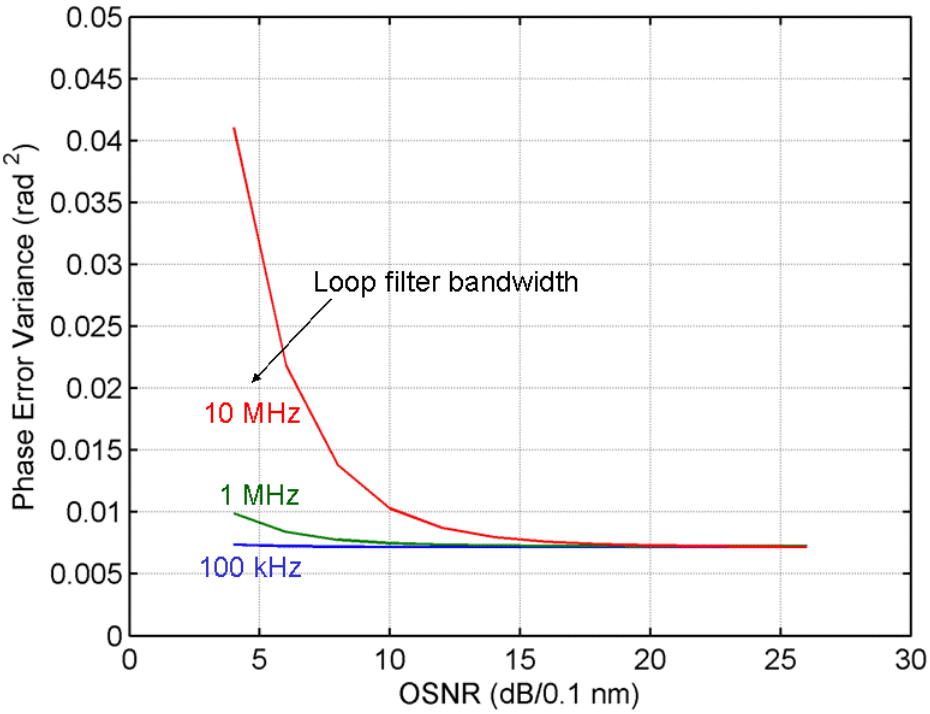

Figure 28: Phase error variance vs OSNR and loop filter bandwidth.

7.2 Non-linear time-domain analysis

The OIPLL has previously been modelled effectively by treating the optical injection locking process as a first-order phase-lock loop, and combining this with a higher order PLL for the electrical loop (see Appendix, Section 7.1 and Reference 2). Most of the modelling has been done in the frequency domain. However, some insight is obtained from a time-domain analysis, and this has also proved to be of use for investigating the response of the OIPLL to a modulated master signal.

The approach and nomenclature of Blanchard [8] is used (Figure 29).

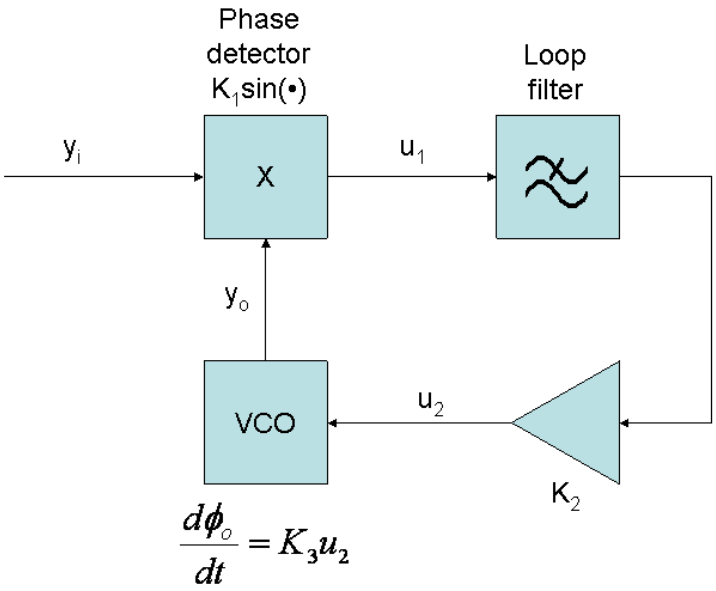

Figure 29: PLL configuration for the time-domain analysis.

The inputs to the phase detector can be written:

$$y_i(t) = A\cos(\omega_i t + \theta_i) = A\sin[\omega_o t + \phi_i(t)]$$
$$y_o(t) = B\cos(\omega_o t + \phi_o)$$

Equation 21

where:

$$\phi_i(t) = \Omega_o t + \theta_i + \frac{\pi}{2}$$
$$\Omega_o = \omega_i - \omega_o$$

The basic loop equations are then given by:

$$u_1(t) = K_1 \sin[\phi_i(t) - \phi_o(t)] = K_1 \sin\phi(t)$$

Equation 22

$$\frac{d\phi_o}{dt} = K_3 u_2(t) = \Omega_o - \frac{d\phi}{dt}$$

Equation 23

To find the relationship between $u_1(t)$ and $u_2(t)$ we consider the loop response in the frequency (Laplace transform) domain. For an OIPLL with a second-order type II loop filter (giving proportional and integral feedback terms:

$$\frac{U_2(s)}{U_1(s)} = K_2\left(\frac{1+s\tau_2}{s\tau_1}\right) + K_{2,OIL}$$

Equation 24

where the optical injection locking has been incorporated as a first-order loop with effective amplifier gain $K_{2,OIL}$.

Thus:

$$\tau_1.sU_2(s) = K_2U_1(s) + K_2\tau_2.sU_1(s) + K_{2,OIL}\tau_1.sU_1(s)$$

Equation 25

so in the time domain

$$\tau_1 \frac{du_2}{dt} = K_2u_1(t) + (K_2\tau_2 + K_{2,OIL}.\tau_1)\frac{du_1}{dt} = \frac{\tau_1}{K_3}\frac{d^2\phi_o}{dt^2}$$

Equation 26

Substituting for $u_1(t)$, and noting that $\frac{d^2\phi_i}{dt^2} = 0$, we obtain:

$$\tau_1 \frac{d^2\phi}{dt^2} + (K\tau_2 + K_{OIL}\tau_1)\cos\phi(t)\frac{d\phi}{dt} + K\sin\phi(t) = 0$$

Equation 27

where

$K = K_1K_2K_3$ and $K_{OIL} = K_1K_{2,OIL}K_3$.

When the loop is locked, $\frac{d\phi}{dt} = 0$, $\frac{d^2\phi}{dt^2} = 0$,

so

$$\sin\phi(t) = 0$$

Equation 28

Hence the static phase error $\phi(t)$ for this loop filter design is zero, independent of the free-running frequency difference between the master and slave lasers Ω_o. The locking limits are determined by the loop DC gain.

7.3 Expressions for Q and BER

7.3.1 Q for coherently detected ASK

In this Appendix, we derive theoretical expressions for the Q factor (giving the BER) for detection of ASK data in the presence of amplified spontaneous emission (ASE) noise. First we consider synchronous coherent detection with perfect phase tracking using a balanced detector, obtaining the local oscillator (LO) – ASE limit performance. Then, a similar expression for the signal – ASE limit performance for direct detection is derived, and subsequently modified to include the effect of ASE – ASE beat noise.

For coherent detection using a balanced receiver, the detected current may be written as (Appendix 7.1, Equation 5):

$$i = R(4\sqrt{P_m P_s}\sin\theta + 2N_{s-ASE})$$

Equation 29

where R is the detector responsivity, P_m is the master (data) signal power, P_s is the slave (local oscillator) signal power and $N_{s\text{-}ASE}$ is the slave-ASE beat noise per detector. For ASK data demodulation we set $\theta = \pi/2$. Writing the mean master signal power as $\overline{P_m}$, the „ones' level, μ_1, and „zeros' level, μ_0, are given by:

$$\mu_1 = 4R\sqrt{2\overline{P_m}P_s}$$

$$\mu_0 = 0$$

Equation 30

The slave-ASE (LO-ASE) beat noise current variance, which is the same for both „ones' and 'zeros' is given by (as Appendix 7.1, Equation 6, with an extra factor of 4 because of the factor of 2 in front of $N_{s\text{-}ASE}$ in Equation 29):

$$\sigma_{s-ASE}^2 = \sigma_1^2 = \sigma_0^2 = 8R^2 P_s P_{ASE}\frac{B_e}{B_o}$$

Equation 31

where P_{ASE} is the total ASE noise power in both polarisations, B_e is the receiver electrical bandwidth, and B_o is the optical bandwidth over which P_{ASE} is spread.

The optical signal-to-noise ratio ($OSNR$), for noise measurements in a 0.1 nm (12.5 GHz) bandwidth, is given by:

$$OSNR = \frac{\overline{P_m}}{P_{ASE}}\frac{Bo}{12.5\,\mathrm{GHz}}$$

Equation 32

Master-ASE (signal-ASE) beat noise and ASE-ASE beat noise are neglected (it is assumed that these are perfectly cancelled in the balanced receiver – see Appendix 7.1), as are other sources of amplitude noise (shot noise, receiver noise, etc.) and phase noise.

The Q is defined as:

$$Q = \frac{\mu_1 - \mu_0}{\sigma_1 + \sigma_0}$$

Equation 33

The LO-ASE limited Q for coherently detected ASK data is thus given by:

$$Q_{LO-ASE} = \frac{\mu_1}{2\sigma_{s-ASE}} = \sqrt{\frac{\overline{P_m}}{P_{ASE}}\frac{B_o}{B_e}} = \sqrt{OSNR\frac{12.5\,\mathrm{GHz}}{Be}}$$

Equation 34

7.3.2 Q for direct detection

For direct detection of ASK (intensity modulated) data using a single-ended detector (direct detection components are cancelled by a balanced receiver):

$$\mu_1 = 2R\overline{P_m}$$

$$\mu_0 = 0$$

Equation 35

To start, we ignore ASE-ASE beat noise. The signal-ASE beat noise current variance is given by:

$$\sigma^2_{sig-ASE} = 2R^2 2\overline{P_m} P_{ASE} \frac{B_e}{B_o}$$

Equation 36

which only occurs in the „ones', i.e.:

$$\sigma_1 = \sigma_{sig-ASE}$$

$$\sigma_0 = 0$$

Equation 37

The signal-ASE limited Q for directly detected ASK data is thus given by:

$$Q_{sig-ASE} = \frac{\mu_1}{\sigma_{sig-ASE}} = \sqrt{\frac{\overline{P_m}}{P_{ASE}} \frac{B_o}{B_e}} = \sqrt{OSNR \frac{12.5\,\mathrm{GHz}}{Be}}$$

Equation 38

i.e. the limiting cases for coherent and direct detection are identical.

However, the assumption that ASE-ASE beat noise is negligible is not realistic, even if a very narrow optical filter (with a bandwidth just adequate to pass the data signal) is used to minimise the ASE power reaching the detector. The ASE-ASE beat noise current variance is given by:

$$\sigma^2_{ASE-ASE} = \frac{n}{2} R^2 P^2_{ASE} \frac{B_e}{B_o} \left(1 - \frac{B_e}{2B_o}\right) \approx \frac{n}{2} R^2 P^2_{ASE} \frac{B_e}{B_o}$$

Equation 39

where n is the number of polarisations of ASE reaching the detector. We will use the approximation on the right of Equation 39, on the assumption that B_o >> B_e.

Including the ASE-ASE beat noise term:

$$\sigma_1^2 = \sigma^2_{sig-ASE} + \sigma^2_{ASE-ASE}$$

$$\sigma_0^2 = \sigma^2_{ASE-ASE}$$

Equation 40

$$Q_{DD} = \frac{\mu_1}{\sqrt{\sigma^2_{sig-ASE} + \sigma^2_{ASE-ASE}} + \sqrt{\sigma^2_{ASE-ASE}}} = \frac{\mu_1}{\sigma_{sig-ASE}\left[\sqrt{1 + \frac{\sigma^2_{ASE-ASE}}{\sigma^2_{sig-ASE}}} + \sqrt{\frac{\sigma^2_{ASE-ASE}}{\sigma^2_{sig-ASE}}}\right]}$$

Equation 41

The ratio of the noise variances is:

$$\frac{\sigma^2_{ASE-ASE}}{\sigma^2_{sig-ASE}} = \frac{n}{8}\frac{P_{ASE}}{\overline{P_m}} = \frac{n}{8}\frac{1}{OSNR}\frac{\mathrm{B_o}}{12.5\,\mathrm{GHz}}$$

Equation 42

Hence

$$Q_{DD} = \frac{\mu_1}{\sigma_{sig-ASE}\left[\sqrt{1 + \frac{n}{8}\frac{1}{OSNR}\frac{\mathrm{B_o}}{12.5\,\mathrm{GHz}}} + \sqrt{\frac{n}{8}\frac{1}{OSNR}\frac{\mathrm{B_o}}{12.5\,\mathrm{GHz}}}\right]}$$

Equation 43

Note that this is $Q_{sig\text{-}ASE}$ reduced by the factor in square brackets. As an example, if we consider $OSNR$ = 10 dB, n = 2, B_o = 1 nm (125 GHz), then Q_{DD} = 0.62 x $Q_{sig\text{-}ASE}$, i.e. ASE-ASE noise leads to a significant reduction in Q.

7.3.3 Theoretical BER vs OSNR

The Q factor is related to the BER by:

$$BER = 0.5\mathrm{erfc}\left(\frac{Q}{\sqrt{2}}\right)$$

Equation 44

where $\mathrm{erfc}(\cdot)$ is the complementary error function. Using the above formulae, we can then easily compare $Q_{LO\text{-}ASE}$ (=$Q_{sig\text{-}ASE}$) and Q_{DD} as a function of OSNR. Examples are shown in Figure 30 for B_o = 1 nm (125 GHz), B_e = 10 GHz and n = 1 and 2. For the experimental conditions (B_o = 1 nm, B_e = 10 GHz and n = 1), the maximum theoretical advantage of coherent detection in terms of OSNR is approximately 2.5 dB at a BER of 10^{-3} and 1.5 dB at a BER of 10^{-9}.

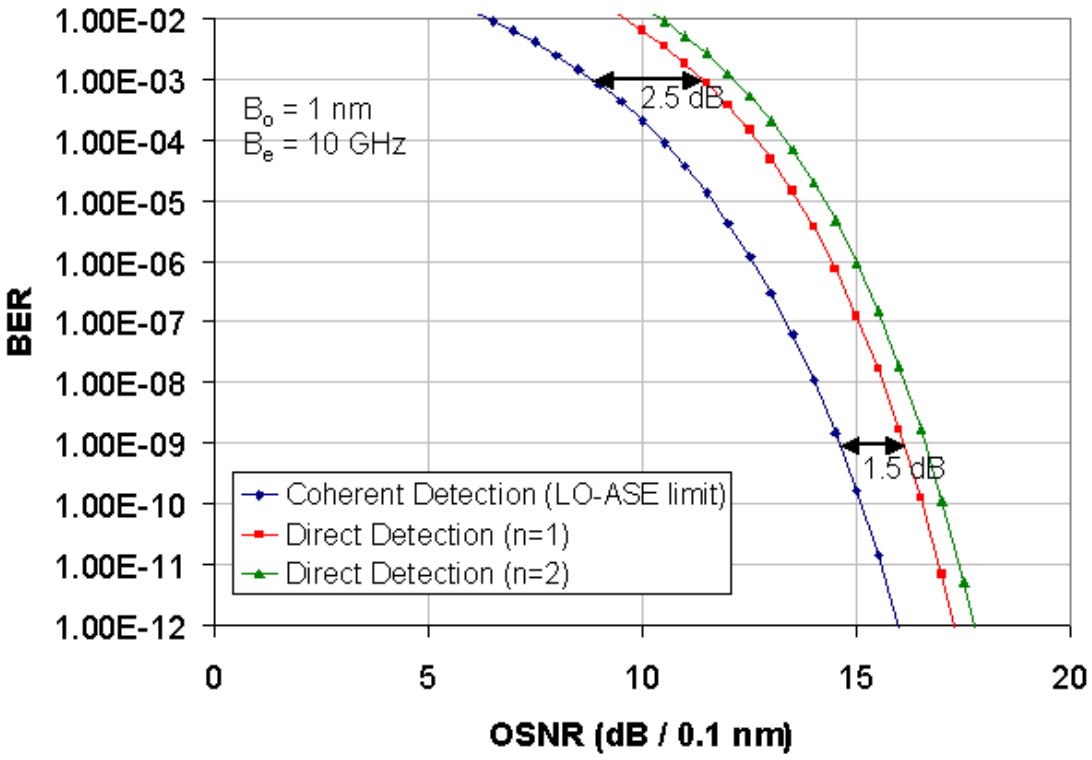

Figure 30: Theoretical BER vs OSNR for coherent and direct detection of ASK data. (n is the number of polarisations of ASE considered.)

7.3.4 Phase noise limited BER

The probability of a Gaussian distribution exceeding $V_{th} = a\sigma$ from the mean is given by:

$$P_e = 0.5\mathrm{erfc}\left(\frac{a}{\sqrt{2}}\right)$$

Equation 45

7.3.4.1 BPSK

In this case assume $V_{th} = 0$. The ONES level is given by $\mu_1\cos\phi_e = a\sigma$, where μ_1 is the ONES level without phase noise and ϕ_e is the phase error.

$$P_{e1} = 0.5\mathrm{erfc}\left(\frac{\mu_1}{\sigma}\frac{\cos\phi_e}{\sqrt{2}}\right)$$

Equation 46

As above (Appendix 7.3.1), for balanced coherent detection (i.e. in the LO-ASE limit):

$$\mu_1 = 4R\sqrt{P_{mean}P_{LO}}$$

Equation 47

$$\sigma^2 = 8R^2P_{LO}P_{ASE}\frac{B_e}{B_o}$$

Equation 48

so

$$\frac{\mu_1}{\sigma} = \sqrt{2}\sqrt{\frac{P_{mean}}{P_{ASE}}\frac{B_o}{B_e}}$$

Equation 49

The OSNR in 0.1 nm is given by:

$$OSNR = \frac{P_{mean}}{P_{ASE}}\frac{Bo}{12.5\text{GHz}}$$

Equation 50

so

$$\frac{\mu_1}{\sigma} = \sqrt{2}\sqrt{OSNR\frac{12.5\text{GHz}}{B_e}} = \sqrt{2}.\sqrt{M}$$

Equation 51

Hence

$$P_{e1} = 0.5\text{erfc}(\sqrt{M}\cos\phi_e)$$

Equation 52

Assuming a Gaussian distribution for ϕ_e, the BER with phase noise is given by:

$$BER_1 = \frac{1}{2\sqrt{2\pi}\sigma_{\phi_e}}\int_{-\infty}^{\infty}\text{erfc}(\sqrt{M}\cos\phi_e)\exp\left(-\frac{\phi_e^2}{2\sigma_{\phi_e}^2}\right)d\phi_e$$

Equation 53

which can be evaluated numerically.

For BPSK the error rate is the same for ONES and ZEROS, so the above integral gives the overall BER.

7.3.4.2 ASK

In this case, define the threshold level V_{th} as a fraction of the ONES level without phase noise. Then for ONES:

$$a\sigma = \mu_1(\cos\phi_e - V_{th})$$

Equation 54

$$\mu_1 = 4R\sqrt{2P_{mean}P_{LO}}$$

Equation 55

As above:

$$\sigma^2 = 8R^2 P_{LO} P_{ASE} \frac{B_e}{B_o}$$

Equation 56

so

$$\frac{\mu_1}{\sigma} = 2\sqrt{\frac{P_{mean}}{P_{ASE}} \frac{B_o}{B_e}} = 2\sqrt{M}$$

Equation 57

Hence

$$P_{e1} = 0.5 erfc(\sqrt{2M}(\cos\phi_e - V_{th}))$$

Equation 58

For ASK zeros, $\mu_0 = 0$ for all ϕ_e, a$\sigma = \mu_1 V_{th}$. So

$$P_{e0} = 0.5 erfc(\sqrt{2M} V_{th})$$

Equation 59

Assuming a Gaussian distribution for ϕ_e, the BER with phase noise for ONES is given by:

$$BER_1 = \frac{1}{2\sqrt{2\pi}\sigma_{\phi_e}} \int_{-\infty}^{\infty} \text{erfc}(\sqrt{2M}(\cos\phi_e - V_{th})) \exp\left(-\frac{\phi_e^2}{2\sigma_{\phi_e}^2}\right) d\phi_e$$

Equation 60

which can be evaluated numerically.

For ZEROS the BER is just $BER_0 = P_{e0}$.

Overall, assuming equal numbers of ONES and ZEROS:

$$BER = 0.5(BER_0 + BER_1)$$

7.4 Active phase control scheme

The vector sum of the E-fields of the master and slave signals at the combining coupler, and hence the voltage from the photodetector, depends on both the locking phase of the optical injection locking process and the relative phase of the signals due to any difference in length between the two paths to the coupler:

$$V_{\text{det}} \propto \sin(\phi_{OIL} + \phi_{\Delta L})$$

Equation 61

where ϕ_{OIL} is the OIL locking phase and $\phi_{\Delta L}$ is the relative phase of the master signal at the coupler, which depends on the path length difference ΔL.

We want to control ϕ_{OIL} (by using the detector voltage, processed by the loop filter, to control the drive current to the slave laser) and $\phi_{\Delta L}$ (by controlling the phase shifter in the master path) independently. To derive an independent control signal for the phase shifter, we use the following scheme.

Expanding V_{det} we have:

$$V_{\det} = \sin\phi_{OIL}\cos\phi_{\Delta L} + \cos\phi_{OIL}\sin\phi_{\Delta L}$$

Equation 62

For optical injection locking, $\sin\phi_{OIL} = \Omega$, where Ω is the normalised free-running frequency detuning, so:

$$V_{\det} = \Omega\cos\phi_{\Delta L} + \sqrt{(1-\Omega^2)}\sin\phi_{\Delta L}$$

Equation 63

When $\phi_{\Delta L}$ is zero, V_{det} is depends linearly on Ω, but for non-zero $\phi_{\Delta L}$ a non-linear dependence on Ω is introduced through the $\sqrt{(1-\Omega^2}$ factor. If we dither Ω by modulating the slave laser current at frequency f_d, then V_{det} will in general contain frequency components at both f_d and $2f_d$. By controlling the phase shifter to minimise the component at $2f_d$, the non-linearity in V_{det} vs Ω will be minimised, i.e. $\phi_{\Delta L}$ will be controlled to be zero.

The frequency deviation of the dither in Ω must be small, and hence the amplitude of the component at $2f_d$ is low, but by using a lock-in amplifier the signal can be recovered and converted to a suitable control signal. By appropriate choice of dither frequency and filter bandwidths, both ϕ_{OIL} and $\phi_{\Delta L}$ can be independently controlled.

8 REFERENCES

[1] M. G. Taylor, “Coherent detection method using DSP for demodulation of signal and subsequent equalization of

[2] A.C. Bordonalli, C. Walton, and A.J. Seeds, “High-performance phase locking of wide linewidth semiconductor lasers by combined use of optical injection locking and optical phase-lock loop,” *J. Lightw. Technol.*, vol. 17, no. 2, pp. 328–342, Feb. 1999.

[3] M. Yoshida, H. Goto, K. Kasai, and M. Nakazawa, “64 and 128 coherent QAM optical transmission over 150 km using frequency-stabilized laser and heterodyne PLL detection,” *Opt. Express*, vol. 16, no. 2, pp. 829–840, Jan. 2008.

[4] M.-S. Kao and J. Wu, “Effect of polarization mode dispersion on a coherent optical system with pilot carrier,” *J. Lightw. Technol.*, vol. 11, no. 1, pp. 303–308, Feb. 1993.

[5] P. J. Anslow, C. R. S. Fludger, S. Savory, I. Hardcastle and J. Fells, “Frequency selective coherent receiver for agile networks,” Proceedings of 32nd European Conference on Optical Communication (ECOC’06), 24-28 September 2006, Cannes, France, vol. 1, pp. 61-62, paper Mo4.2.4.

[6] N.A. Olsson, “Lightwave systems with optical amplifiers,” *J. Lightw. Technol.*, vol. 7, no. 7, pp. 1071–1082, Jul. 1989.

[7] F.M. Gardner, “Phaselock Techniques,” 2nd edition, Wiley, 1979.

[8] A. Blanchard, “Phase-locked loops: application to coherent receiver design,” Wiley-Interscience, New York, 1976.